NATIONAL ADVISORY COMMITTEE FOR AERONAUTICS

WARTIME REPORT

ORIGINALLY ISSUED
June 1945 as
Advance Restricted Report L5F01a

EFFECT OF FABRIC DEFLECTION AT HIGH SPEEDS ON THE AERODYNAMIC CHARACTERISTICS OF THE HORIZONTAL TAIL SURFACE OF AN SB2D-1 AIRPLANE

By Carl F. Schueller and Peter F. Korycinski

Langley Memorial Aeronautical Laboratory
Langley Field, Va.

NACA

WASHINGTON

NACA ARR No. L5F01a

NATIONAL ADVISORY COMMITTEE FOR AERONAUTICS

ADVANCE RESTRICTED REPORT

EFFECT OF FABRIC DEFLECTION AT HIGH SPEEDS ON THE AERODYNAMIC CHARACTERISTICS OF THE HORIZONTAL TAIL SURFACE OF AN SB2D-1 AIRPLANE

By Carl F. Schueller and Peter F. Korycinski

SUMMARY

Results are presented of an investigation of a full-scale horizontal tail surface to determine the elevator-fabric deflection at high speeds and the aerodynamic effects of the fabric deflection. Two fabric-covered elevators, differing only in rib spacing, and a solid wooden elevator were tested. The first elevator had a rib spacing of approximately 4 inches. The second elevator had a rib spacing of approximately 8 inches, which is more nearly typical of the spacing currently used. Tests were carried to a maximum Mach number of 0.68 except for model configurations for which the maximum allowable loads were reached at lower speeds.

No appreciable fabric deflections occurred for the elevator with 4-inch rib spacing. A maximum fabric bulge of 0.6 inch between ribs was measured for the elevator with 8-inch rib spacing at a Mach number of 0.55, an elevator angle of -3.7°, and an angle of attack of 9.7°. Local failures of the fabric attachment to the elevator ribs occurred. By moving the elevator vent holes from the vicinity of the trailing edge to the leading edge, the bulge was eliminated for these test conditions at the expense, however, of some increase in fabric depression on the pressure side of the elevator.

Marked increases in the elevator hinge-moment coefficients occurred as the test Mach number was increased. For the elevator with 4-inch rib spacing the hinge-moment parameter C_{h_δ} (rate of change of hinge-moment coefficient with elevator deflection) increased from a value at low speed of -0.005 to a value of -0.009 at a Mach number of 0.68. The effect of fabric deflection for the

elevator with 8-inch rib spacing caused an additional adverse increment in hinge-moment coefficient as the speed was increased. The effectiveness of the elevator with 4-inch rib spacing did not change appreciably with Mach number. As a result of fabric deflection, however, the effectiveness of the elevator with 8-inch rib spacing decreases sharply at Mach numbers above 0.56. The adverse effect of fabric deflection on elevator hinge moment was decreased slightly by locating the vent holes in the leading edge rather than at the trailing edge of the elevator.

INTRODUCTION

Tests were made to determine the effects of elevator-fabric deflections at high speeds and of compressibility on the aerodynamic characteristics of a full-scale horizontal tail surface. The necessity of such an investigation has been demonstrated by the excessive and irregular hinge moments encountered during high-speed maneuvers and by numerous instances of control-surface failure on some of the more recent high-speed airplanes equipped with fabric-covered control surfaces.

The present report gives the results of tests on three elevators with identical external dimensions. Elevators 1 and 2 were fabric covered, had rib spacings of approximately 4 and 8 inches, respectively, and were used to determine the fabric deflection. The third elevator was made of solid mahogany, included two rows of pressure orifices, and was used to determine the external pressure distribution. Each elevator was tested through ranges of Mach number of 0.2 to 0.68, elevator angle of 9° to -9°, and stabilizer angle of 0° to 9°. Tests of any combination of the aforementioned variables were limited by the maximum allowable loads. In addition, elevator 2 was tested with the original vents sealed and vents at the leading edge or at 10 percent elevator chord c_e to determine the effect of vent location on fabric deflection.

The tests were conducted at the Langley 16-foot high-speed tunnel, Langley Memorial Aeronautical Laboratory.

COEFFICIENTS AND SYMBOLS

C_D	drag coefficient (D/qS)
C_h	hinge-moment coefficient $(H/q\bar{c}_e^2 b)$
C_L	lift coefficient (L/qS)
C_m	pitching-moment coefficient $\left(\frac{M_{c'/4}}{qSc'}\right)$
D	drag of entire model
H	hinge moment
L	lift of entire model
$M_{c'/4}$	pitching moment about quarter-chord point of mean aerodynamic chord
b	span, feet
c	chord of horizontal tail surface except when designated otherwise by subscript, feet
c'	mean aerodynamic chord of horizontal tail
$\bar{c}_e$	root-mean-square of elevator chord behind hinge line
q	dynamic pressure $\left(\frac{1}{2}\rho V^2\right)$
ρ	mass density of air, slugs per cubic foot
V	velocity, feet per second
S	total model area, square feet
M	Mach number
P	pressure coefficient $\left(\frac{p - p_o}{q_o}\right)$
p	static pressure at any point
α	angle of attack of stabilizer, ~~degrees~~
δ	angle of elevator chord with respect to stabilizer chord, degrees
$\frac{\partial\alpha}{\partial\delta}$	elevator-effectiveness parameter $\left(\frac{C_{L_\delta}}{C_{L_\alpha}}\right)$

Parameters:

$$c_{L_\alpha} = \left(\frac{\partial C_L}{\partial \alpha}\right)_\delta$$

$$c_{L_\delta} = \left(\frac{\partial C_L}{\partial \delta}\right)_\alpha$$

$$c_{h_\alpha} = \left(\frac{\partial C_h}{\partial \alpha}\right)_\delta$$

$$c_{h_\delta} = \left(\frac{\partial C_h}{\partial \delta}\right)_\alpha$$

The subscripts outside the parentheses represent the factors held constant during the measurement of the parameters.

Subscripts:

b balance

e elevator

f flap (elevator + balance)

i internal

o free stream

APPARATUS AND METHODS

Test model.- The model was a full-scale left-hand horizontal tail surface of the SB2D-1 airplane. The airfoil section used was based on the NACA 0020-64 airfoil profile modified to have a maximum thickness ratio of 10.7 percent and a straight taper behind the 63-percent-chord station. Since a semispan model was used, it was necessary to locate the center line of the airplane in the plane of the tunnel wall to produce air-flow conditions corresponding to those of flight. This result was accomplished by adding a 20.5-inch stub wing to the tail surface. Figure 1 shows the model installed in the tunnel and figure 2 presents the physical characteristics of the model.

The stabilizer was metal covered and included a fabric seal to prevent air from flowing between the rear part of the stabilizer and the elevator leading edge. (See fig. 3.) The model was not aerodynamically smooth. Brazier head rivets, access and inspection doors, and considerable waviness characterized the stabilizer surface.

Each elevator had a modified elliptical nose and a straight taper behind the hinge line ending in a trailing-edge angle of 12°. The coordinates for the elevator contour are presented in figure 3. Elevators 1 and 2 were of metal construction and fabric covered. Details of the rib locations are shown in figure 4. The average rib spacings are approximately 4 and 8 inches for elevators 1 and 2, respectively. Both elevators had one $\frac{3}{8}$-inch-diameter drain hole in each elevator panel on the lower surface approximately 1 inch from the elevator trailing edge. Since each elevator panel had one hole, these openings also served as air vents. Elevator 3 was made of solid mahogany and was dimensionally equal to elevators 1 and 2. Two rows of pressure orifices on the upper and lower surfaces, 33 and 70 inches from the longitudinal center line of the airplane, were built into this elevator.

Hinge-moment measurement.- Figure 5 is a schematic view of the model installation and illustrates the apparatus used to measure the elevator hinge moment. This sketch shows the extended elevator torque tube passing through a hole in the side of the tunnel and into two self-alining bearings mounted on the tunnel balance frame. The elevator hinge moment was transferred through the elevator torque tube to a 10-inch crank and then through a jackscrew to the scale platform. The jackscrew was also used to vary the elevator angle. The platform scale was attached rigidly to the tunnel balance frame and, since all other related parts were also attached to the tunnel balance frame, hinge-moment measurements could not interfere with the measurements of lift, drag, and pitching moment. All force and moment data were recorded simultaneously.

Fabric-deflection measurements.- Stripes $\frac{1}{4}$-inch wide were painted chordwise on both surfaces of the fabric-covered elevators to permit the measurement of the fabric

deflection. (See fig. 1.) Solid stripes were painted over each rib and broken stripes midway between the ribs, on the upper and lower surfaces. These stripes are straight and parallel for the static condition (see fig. 6) but because of air loads the fabric deflects and the stripes bend. Cameras in fixed positions were provided to photograph the elevator surfaces simultaneously and thus provide records of the fabric deflection. The deflection of the painted stripes was measured from enlargements of the photographs.

Fabric-tension measurements.- The fabric tension for each elevator panel was measured with an instrument designed by the Flight Research Division of the Laboratory. A detailed description of the instrument and the technique of measurement are given in reference 1. The fabric tensions were measured before and after the tests to determine any change in fabric tension resulting from repeated stresses that were applied to the fabric during testing. Table I presents a summary of the measurements and indicates that the change in fabric tension for elevator 1 is within the accuracy of the measurements. Elevator 2 had a slightly lower fabric tension after testing, but this difference may be a temperature or humidity effect.

Pressure measurements.- The pressure distribution over the elevator was obtained with elevator 3, which contained two rows of orifices. The external pressures over the upper surface of the stabilizer were obtained by the use of two pressure belts located at the 33-inch and 70-inch stations. All stations were measured in inches from the longitudinal center line of the airplane.

Two 0.050-inch-diameter tubes were installed in elevators 1 and 2 at the 47-inch and 97-inch stations to measure the elevator internal pressure.

TEST PROCEDURE

The general procedure in conducting the tests was to set the desired angle of attack and elevator angle at the beginning of each test. Data were then recorded at each of the following speeds: Mach number = 0.20, 0.35, 0.45, 0.50, 0.55, 0.60, 0.65, and 0.68 or until the maximum allowable load on the tail surface was attained.

The stabilizer root angle remained fixed during the test. The elevator root angle was measured and recorded at each test point, since it varied slightly because of twist of the torque tube and deflection of the scale platform. The angles of attack and elevator angles are believed to be accurate within ±0.1°.

REDUCTION OF DATA

Force data.- The lift, drag, and pitching-moment coefficients presented in this report are based on the wing area of the complete model (see fig. 2) including the stub wing. All data were taken with the elevator seal in, the elevator vents at the trailing edge, and the trim tab neutral, unless specified otherwise.

The force data were corrected for tunnel-wall effects by the use of the reflection-plane theory given in reference 2. The model thickness was such a small part of the tunnel diameter that tunnel blockage corrections were negligible. Since the elevator torque tube could twist and the scale platform deflect, the elevator angle changed with hinge moment. Calibrations of the twist of the elevator torque tube and the deflection of the scale platform with elevator hinge moment were used to correct the indicated elevator angles to actual angles. The corrected data were cross-plotted and the values at selected angles of attack and elevator angle were then plotted against Mach number. Since a large part of the data presented is plotted against Mach number, figure 7 has been included to show the average dynamic pressures and the average Reynolds numbers corresponding to the test Mach numbers. The Reynolds number is based on the assumed mean aerodynamic chord of 4.41 feet. It should be mentioned that the changes which occur with speed are not pure Mach number effects but include effects due to distortion of the model under load. The effects shown therefore apply only to the particular combination of dynamic pressure and Mach number tested herein. The results, however, are plotted against Mach number, and the dynamic pressure at any Mach number may be obtained from figure 7.

Fabric deflection.- A special film viewer was used to enlarge the photographic negatives of the elevator surfaces. Vertical scales were attached to the elevator surfaces at each broken stripe and photographed for all

model configurations to obtain films of the static condition (zero deflection). A quantitative measure of the fabric deflection was obtained by comparing a photograph for the static condition (zero deflection) with one made during a test. The displacement of any stripe was then measured and recorded.

RESULTS AND DISCUSSION

Fabric Deflection

Elevator 1.- Figure 8 is a photograph of the fabric deflection on the upper surface of elevator 1 (4-inch rib spacing) at $\alpha = 0^\circ$, $\delta = 4.2^\circ$, and $M = 0.66$. The fabric deflection is not appreciable at any point along the elevator except for a small bulge occurring near the inboard hinge. No other photographs are shown for this elevator because the fabric deflection was not serious during any of the tests with this elevator.

Elevator 2.- Figure 9 is a photograph of the fabric deflection of both surfaces of elevator 2 (8-inch rib spacing) at $\alpha = 0^\circ$, $\delta = 3.3^\circ$, and $M = 0.55$. Considerable bulge occurred on the top surface behind the hinge line. This bulge changed to depression on the rear part of the elevator. Since the fabric was sewed to the elevator ribs, the solid stripes should show no deflection. A number of solid stripes, however, are deflected. (See fig. 9(a).) Deflection of the solid stripes indicates failure of the fabric attachment at these points and is the beginning of a condition that would result in complete failure of the surface if the air loads were increased. Figure 10 is a photograph of the fabric deflection at $\alpha = 3^\circ$, $\delta = -0.7^\circ$, and $M = 0.62$. In general, the upper surface is slightly bulged just behind the hinge line. The most serious bulge occurs at the inboard hinge and is believed to be a result of weak fabric attachment around the hinge-pocket cut-out rather than of local-suction peak pressures. Figure 10 also shows the fabric pulled away from the ribs. (Note solid stripes.)

Figures 11, 12, and 13 are plots showing the variation of the fabric deflection with percent of elevator chord and include only the portion of the elevator chord for which the fabric was deflected; therefore only the end points of zero deflection are shown. These data are

for a representative spanwise station (77.1-inch station). Figure 11 presents the fabric deflection for various Mach numbers at elevator angles averaging -1.5° and $\alpha = 0^\circ$. Although the elevator angle changed slightly (0.5°) with speed, it is apparent from figure 11 that increasing the speed increases the fabric deflection. The maximum fabric deflection of the lower surface has been plotted separately for each speed in figure 14 and shows that the fabric deflection varies linearly with dynamic pressure for elevator 2 at $\alpha = 0^\circ$ and $\delta = -1.5^\circ$. Figure 12 presents the fabric deflection for various elevator angles at $\alpha = 0^\circ$ and $M = 0.55$. Increasing the elevator angle negatively increases the fabric bulge on the lower surface while the deflection of the upper surface changes from bulge to depression. Figure 13 presents the fabric deflection for various angles of attack at $M = 0.55$ and $M = 0.53$. The maximum fabric deflection attained during these tests was a 0.6-inch bulge on the lower surface of elevator 2 at $\alpha = 7.9^\circ$, $\delta = -3.7^\circ$, and $M = 0.55$ (fig. 13).

Pressure distribution.- Fabric bulge tends to be unstable since it causes an increase in the local negative pressures, which in turn cause an increase in the fabric bulge. This adverse effect is magnified at high speeds and has been observed to result in failure of the fabric attachments to the elevator structure and finally complete failure of the fabric. An investigation to determine the external pressure distribution over the elevators and the location of air vents that would result in negative internal pressures and a reduction in elevator fabric bulge was therefore undertaken. Elevator 3, which was dimentionally equal to elevators 1 and 2, was tested for this purpose.

The tests of elevator 3 indicated that the pressure distributions at the 33-inch and 70-inch stations were very nearly the same on the elevator but differed appreciably near the stabilizer leading edge. This difference may be attributed to surface irregularities. Removing the elevator seal increased slightly the positive pressures on the lower surface of the elevator balance area for positive elevator angles but had little effect on the pressures over the other portions of the elevator. The external pressure distributions at $M = 0.20$ and the 33-inch station for three elevator angles are presented in figures 15, 16, and 17 for $\alpha = 0^\circ$, 3°, and 6°, respectively. These figures indicate that vents in

both the upper and lower surfaces at the elevator leading edge or at approximately 10 percent of the elevator chord behind the hinge line c_e will result in negative average internal pressures. Although the average pressures at these points are not the most negative, they are consistently negative and are least affected by changes in elevator angle.

Effect of various vent locations for elevator 2.- The original elevator vents were sealed, and the effect on internal pressure and fabric deflection of the elevator as a result of locating a vent in each elevator panel at the leading edge or at 10 percent of c_e on the upper and lower surfaces was determined. The variation of the internal pressure of the elevator with elevator angle is presented in figure 18 for three vent configurations. A comparison of these curves shows that the average internal pressure coefficient P_i for the original vent configuration is changed from -0.02 to -0.08 for vents at 10 percent of c_e and to -0.23 for vents at the elevator leading edge.

Figure 19 presents quantitative comparisons of the fabric deflection along the elevator chord for the three vent locations at $\alpha = 0^\circ$, $\delta = 4^\circ$, and $M = 0.55$. The maximum bulge on the upper surface is reduced from 0.4 inch for the original vent configuration to 0.2 inch by using vents at 10 percent of c_e and to 0.26-inch depression with vents at the elevator leading edge. No measurements were made for the lower surface with vents at 10 percent of c_e but visual observation indicated that the fabric was depressed for this condition, as would be expected.

Figure 20 is a photograph of the fabric deflection with vents at the elevator leading edge for $\alpha = 0^\circ$, $\delta = 4^\circ$, and $M = 0.55$. Comparison of figures 20 and 9 shows that the upper-surface bulge is changed to depression with vents at the elevator leading edge, except for a small local bulge at the upper surface near the inboard hinge. It is apparent from figures 19 and 20 that location of the vents at the elevator leading edge will eliminate the danger of the fabric pulling loose from the ribs and failing for elevator angles up to at least 4°.

Aerodynamic Characteristics

Basic data.- The lift, drag, pitching-moment, and hinge-moment coefficients are plotted against Mach number in figures 21 and 22 for elevators 1 and 2, respectively. These data are presented for $\alpha = 0^\circ$, 3°, 6°, and 9°, and a maximum range of $\delta = 6^\circ$ to -9°. The fact that the C_L, C_m, and C_{h_e} values for $\alpha = 0^\circ$ and $\delta = 0^\circ$ are not zero is due either to asymmetry of the model or to small errors in setting the neutral angle of the stabilizer, elevator, or trim tab.

The increase in the lift or pitching-moment coefficient with Mach number for both elevators is less than the increase predicted by Glauert's factor $(1 - M^2)^{-1/2}$. This difference is believed to be a result of the twisting of the stabilizer and elevator toward their zero angles due to the aerodynamic loads. The drag-coefficient curves show the usual large increases in the vicinity of the critical Mach numbers. The data show pronounced increases in elevator hinge-moment coefficient with increasing Mach number. Integration of the elevator pressure-distribution diagrams showed increases of approximately the same magnitude. The rate of increase of hinge moment with Mach number was more than twice as great as would be predicted by the use of the Glauert factor. In general, the changes in the aerodynamic coefficients with Mach number were gradual and consistent. The critical Mach numbers for the various model configurations could not be greatly exceeded in these tests and consequently the abrupt and drastic changes that have been noted in tests of small models at high supercritical speeds were not encountered. The only indication of such changes occurred for elevator 2 near the highest test speeds. (See figs. 23 and 24.)

Variation of lift with α and δ.- The variation of the lift-curve-slope parameter C_{L_α} with Mach number for elevators 1 and 2 is presented in figure 23. The slopes were measured from plots of C_L against α in the region of $\alpha = 0^\circ$ to 3°. The values at low speed of C_{L_α} are considerably lower than the value estimated from two-dimensional data for a wing of this section and plan form, principally because of the discontinuity of the airfoil contour at the stabilizer trailing edge and the elevator leading edge.

The change in C_{L_δ} with Mach number for elevators 1 and 2 is shown in figure 24 and indicates good agreement between the two elevators at low speeds. For elevator 1, C_{L_δ} increases gradually with speed. At the maximum Mach number attainable (0.68), the data indicate that C_{L_δ} was beginning to decrease. The variation of C_{L_δ} with Mach number for elevator 2 indicates a marked adverse effect of fabric deflection at Mach numbers above 0.60.

Elevator effectiveness.- The variation of the elevator-effectiveness parameter with Mach number is shown in figure 25 for elevators 1 and 2. The curves show a small decrease in effectiveness as the speed is increased from $M = 0.20$ to $M = 0.45$. Beyond Mach numbers of 0.45 the effectiveness for both elevators increases. The effectiveness of elevator 1 is still increasing at $M = 0.68$ but falls off sharply beyond values of $M = 0.56$ for elevator 2. Since elevator 1 had negligible fabric deflection and elevator 2 had serious fabric deflection, the adverse effect shown is a result of fabric deflection. The theoretical effectiveness for a plain flap hinged at its leading edge has been computed according to the thin-airfoil theory (see reference 3) and is shown in figure 25. The actual elevator effectiveness is approximately 71 percent of the theoretical value for a plain flap at moderate speeds.

Pitching moment.- The variation of the pitching-moment parameter $\partial C_m/\partial C_L$ with Mach number is shown in figure 26 for elevators 1 and 2. The value of this parameter is approximately the position of the aerodynamic center of the airfoil with respect to the quarter-chord point of the assumed mean aerodynamic chord (fig. 2). The change in the center-of-lift position caused by elevator deflection is given by the parameter $(\partial C_m/\partial C_L)_\alpha$. The variation of this parameter with Mach number was about the same for both elevators; that is, the center of lift was shifted rearward. The change in the center-of-lift position caused by angle of attack is given by the parameter $(\partial C_m/\partial C_L)_\delta$. Increasing the Mach number caused a greater increase in this parameter for elevator 2 than for elevator 1, probably as a result of the fabric deflection on elevator 2.

Hinge moment.- The change in C_{h_α} with Mach number is shown in figure 27 for elevators 1 and 2. In general, the agreement of the data for the two elevators is good, although an almost constant small difference exists between the values for the two elevators. Small differences in contour between the two elevators could cause this difference. The small low-speed value of C_{h_α} (-0.001) decreased about 70 percent between $M = 0.20$ and $M = 0.60$.

The variation of C_{h_δ} with Mach number is shown in figure 28. Large increases in the negative values of C_{h_δ} occurred with increasing speed for elevators 1 and 2. The value of C_{h_δ} for elevator 1 (4-inch rib spacing) increased from -0.005 to -0.009 between $M = 0.20$ and $M = 0.68$. The difference between the low-speed values of C_{h_δ} for the two elevators is believed to be caused by minor physical differences such as a small bump that existed on the upper surface of elevator 2. This bump was 5.5 percent of the elevator thickness, was located at 6.5 percent of the total elevator chord from the nose, and tapered to zero at the elevator leading edge and at the hinge line. Figure 28 also shows curves for elevators having zero and 100-percent aerodynamic balance. The curve for zero aerodynamic balance was calculated according to thin-airfoil theory (reference 3) for a plain flap hinged at its leading edge. Elevator 1 had 50-percent aerodynamic balance at $M = 0.20$ but, because of the adverse Mach number effects, the balance was reduced to 8 percent at $M = 0.68$. The control forces required for such an elevator would thus approach those that would be obtained with an ordinary unbalanced flap, when it is assumed that the value of C_h for such a flap does not change with Mach number. In the absence of boundary-layer changes, it might logically be assumed that the elevator hinge moment would increase with speed according to Glauert's factor. The low-speed value has been increased according to this factor $(1 - M^2)^{-1/2}$ and the data are plotted in figure 28. A comparison of the two curves shows that the rate of increase in C_{h_δ} with Mach number is about double the rate of increase predicted by Glauert's factor. Elevator 2 had 43-percent aerodynamic balance at $M = 0.20$ but zero aerodynamic balance at $M = 0.60$. The increase in C_{h_δ} is markedly greater for elevator 2 than for elevator 1 because of the adverse effect of fabric deflection. The

difference in the increases of C_{h_δ} with Mach number for the two elevators appears to be an effect of fabric deflection, since fabric deflection was the principal difference between the two elevators. This difference is plotted at the top of figure 28. The effect of fabric deflection on C_{h_δ} was to cause an increase of -0.002 from $M = 0.20$ to $M = 0.60$. This increase was about 40 percent of the low-speed value of C_{h_δ} for the elevator tested. An increase of this magnitude would be still more serious for a highly balanced tail surface for which the initial C_{h_δ} might be of the order of -0.001.

Effect of vents on hinge moment.- As was shown in figure 19, the fabric deflection varies with vent location. The best vent location from a consideration of safe fabric deflection was found to be at the elevator leading edge. Figure 29 shows the variation of the hinge-moment coefficient with elevator angle, at $M = 0.55$, for the three vent locations tested and with all vents sealed. The data presented in this figure show that the vents located at the elevator leading edge produced the smallest value of C_{h_δ}. The beneficial effect of vents at the leading edge (reduced internal pressure) is probably a result of changing the asymmetrical elevator-surface deflections, which resulted in appreciable elevator camber, to more symmetrical deflections with less camber. (See fig. 19 and reference 4.)

Effect of elevator seal.- A limited amount of data with the elevator seal removed was obtained over a small range of elevator angle at $\alpha = 0^\circ$. These data indicated no appreciable effect of the seal on the elevator hinge moment.

Tab effectiveness.- The effectiveness of the elevator trim tab through the speed range is shown in figure 30. The data for a tab angle of -10° show a gradual decrease in effectiveness with increasing speed - the ΔC_h decreasing from 0.044 at $M = 0.20$ to 0.030 at $M = 0.65$. The effectiveness remains approximately constant from $M = 0.20$ to $M = 0.60$ for a tab angle of 8.8°.

CONCLUSIONS

An investigation of the characteristics of a full-scale horizontal tail with fabric-covered elevators at

Mach numbers ranging from 0.20 to 0.68 has led to the following conclusions:

1. Elevator 1 (4-inch rib spacing) had no appreciable fabric deflection in the speed range of these tests. Elevator 2 (8-inch rib spacing) had a maximum fabric bulge of 0.6 inch between ribs at a Mach number of 0.55, an elevator angle of -3.7°, and an angle of attack of 9.7°. Local failures of the fabric attachment to the elevator ribs occurred with elevator 2.

2. Vent holes located at the elevator leading edge on either side of the seal, rather than in their original position on the lower surface near the trailing edge, eliminated the bulge for a moderate range of elevator angle at the expense, however, of some increase in fabric depression on the pressure side of the elevator.

3. Elevators 1 and 2 produced very large increases in elevator hinge-moment coefficient as the Mach number was increased. The value of C_{h_δ} (the slope of the curve of hinge moment against elevator deflection) for elevator 1 (4-inch rib spacing) increased from -0.005 to -0.009 between Mach numbers of 0.20 to 0.68.

4. In addition to the increase in hinge moment resulting from increasing speed, elevator 2 (8-inch rib spacing) had an increase in hinge moment due to fabric deflection. The fabric deflection for this elevator increased the value of C_{h_δ} by -0.002 at a Mach number of 0.60. Fabric deflection also caused an early loss in elevator effectiveness. Elevator 1 maintained its effectiveness up to the maximum test speed (a Mach number of 0.68) but the effectiveness of elevator 2 decreased sharply at Mach numbers above 0.56.

5. The adverse effect of fabric deflection on elevator hinge moment was decreased slightly by locating the vent holes in the leading edge rather than at the trailing edge of the elevator.

Langley Memorial Aeronautical Laboratory
National Advisory Committee for Aeronautics
Langley Field, Va.

REFERENCES

1. Neihouse, A. I., and Kemp, W. B.: Effect of Fabric Deflection on Rudder Hinge-Moment Characteristics as Determined by Wind-Tunnel Tests. NACA ARR No. I5A24, 1945.

2. Swanson, Robert S., and Toll, Thomas A.: Jet-Boundary Corrections for Reflection-Plane Models in Rectangular Wind Tunnels. NACA ARR No. 3E22, 1943.

3. Perring, W. G. A.: The Theoretical Relationships for an Aerofoil with a Multiply Hinged Flap System. R. & M. No. 1171, British A.R.C., 1928.

4. Mathews, Charles W.: An Analytical Investigation of the Effects of Elevator-Fabric Distortion on the Longitudinal Stability and Control of an Airplane. NACA ACR No. L4E30, 1944.

TABLE I

ELEVATOR FABRIC TENSIONS

[Accuracy of measurement, ±0.2 lb/in.]

Test condition	Tension (lb/in.)			
	Upper surface		Lower surface	
	Max.	Min.	Max.	Min.
Elevator 1				
Before testing	7.4	6.3	8.6	6.8
After testing	7.6	6.7	8.8	7.6
Elevator 2				
Before testing	7.2	5.2	7.5	6.8
After testing	7.0	6.0	6.7	6.0

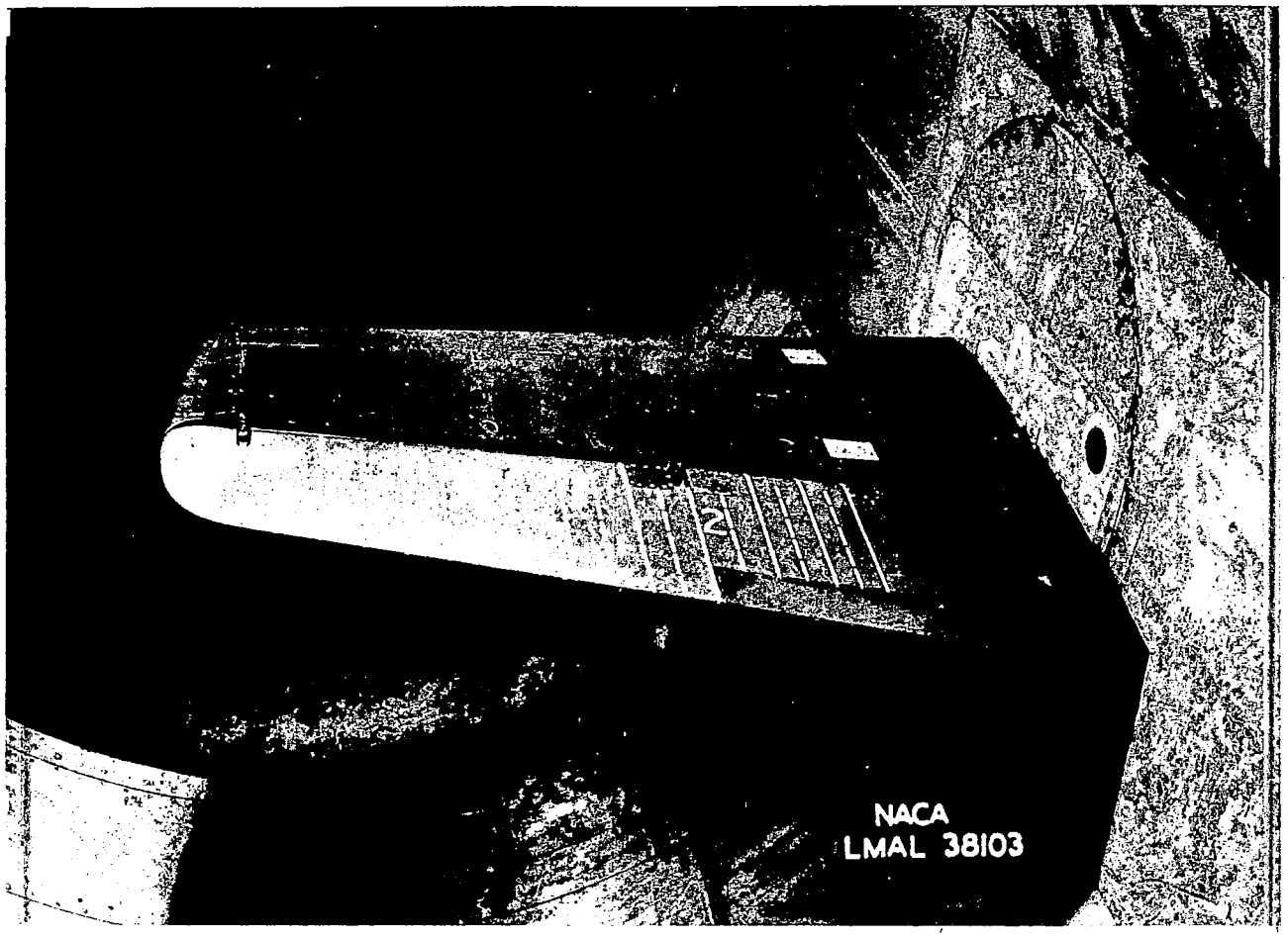

Figure 1.- General view of SB2D-1 semispan horizontal tail installed in Langley 16-foot high-speed tunnel.

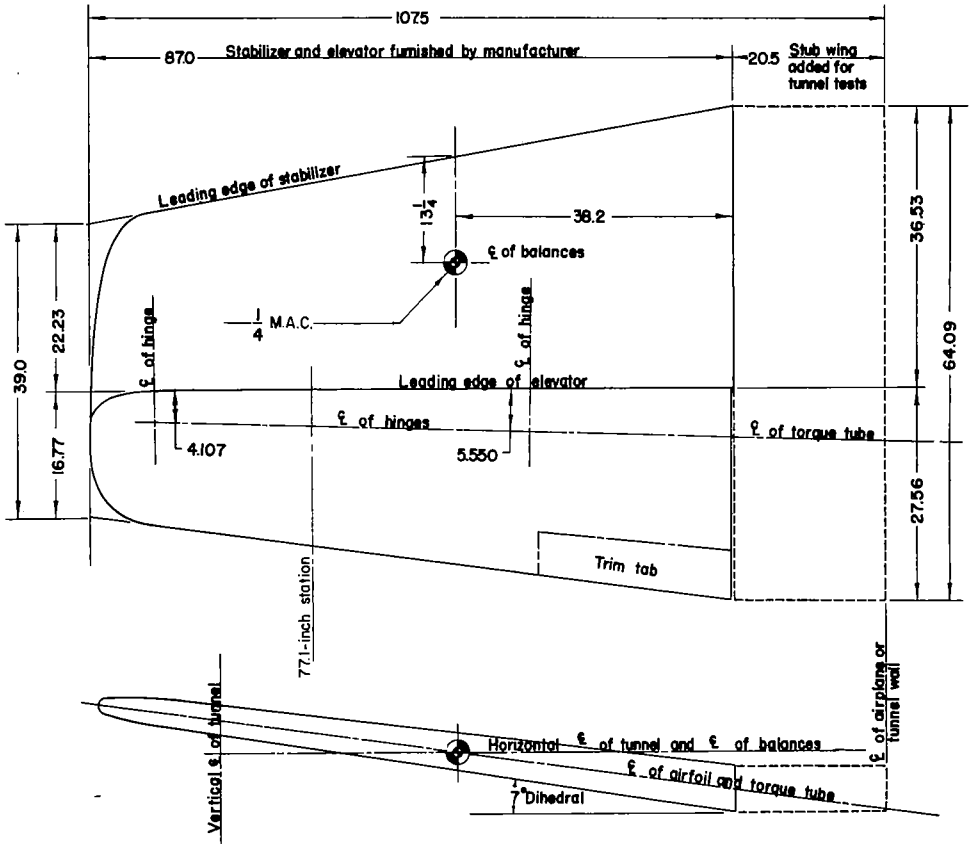

Root-mean-square of elevator chord behind hinge line	17.17 in.
Area of stabilizer	2522 sq in.
Area of elevator	1905 sq in.
Total area of horizontal tail including stub section	5741 sq in.
Area of tab	129.5 sq in.
Aspect ratio	4.0

NATIONAL ADVISORY COMMITTEE FOR AERONAUTICS

Figure 2.- General arrangement of the horizontal tail surface.

(All dimensions shown are measured in the plane of the section and are in inches)

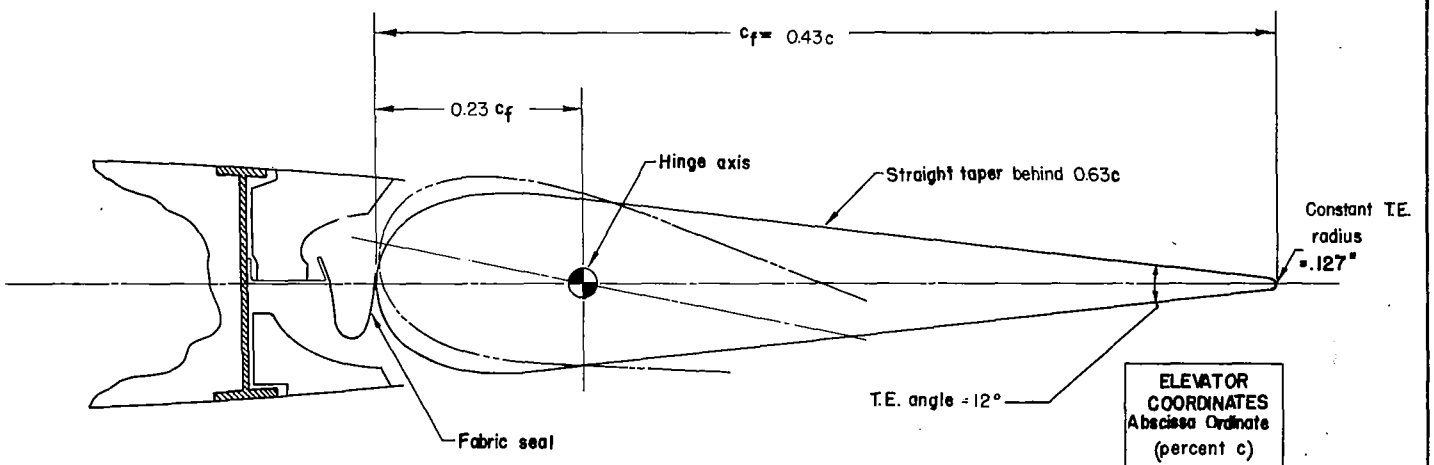

ELEVATOR COORDINATES	
Abscissa (percent c)	Ordinate
0.50	3.60
1.00	4.17
2.00	5.57
3.00	6.51
4.00	7.20
5.00	7.73
6.00	8.14
8.00	8.71
10.00	9.02
12.00	9.16
14.00	9.12
16.00	8.97
23.00	8.26
L.E. Rad.=10.88	

NATIONAL ADVISORY COMMITTEE FOR AERONAUTICS

Figure 3.- DETAIL OF ELEVATOR AND SEAL.

(0020-64 AIRFOIL MODIFIED TO MAXIMUM THICKNESS OF 10.71 PERCENT.)

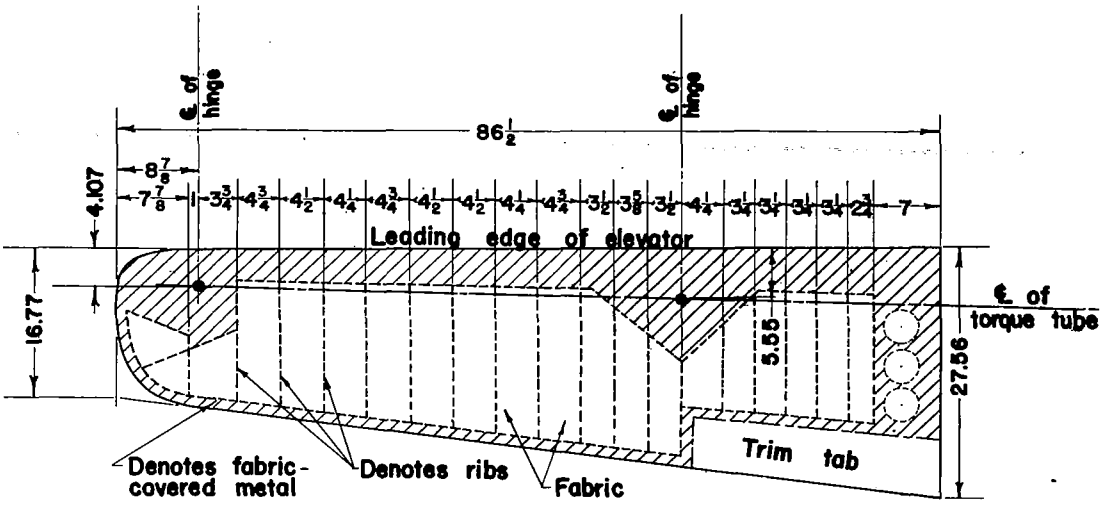

ELEVATOR 1

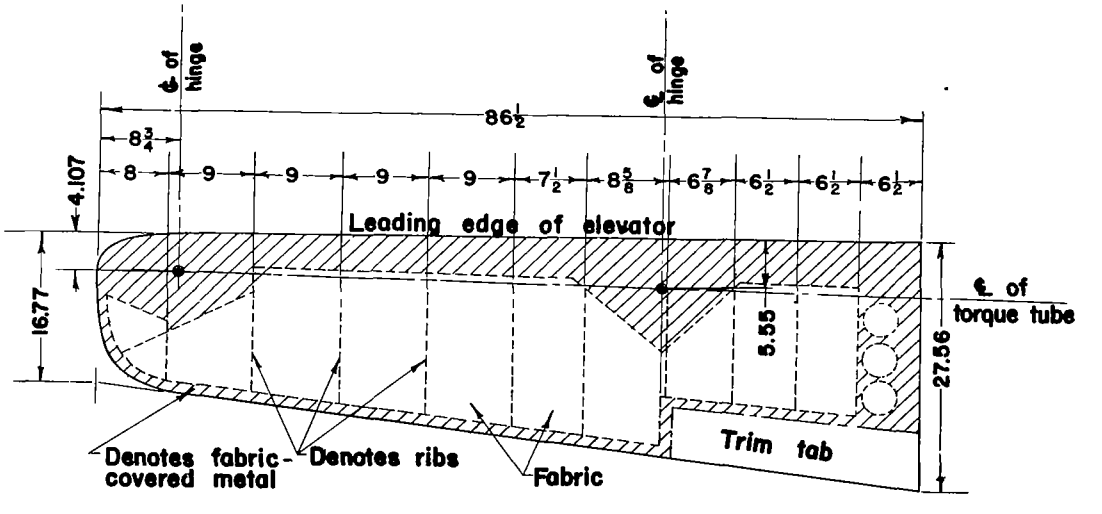

ELEVATOR 2

NATIONAL ADVISORY COMMITTEE FOR AERONAUTICS

FIGURE 4.—RIB SPACING FOR THE TWO FABRIC-COVERED ELEVATORS.

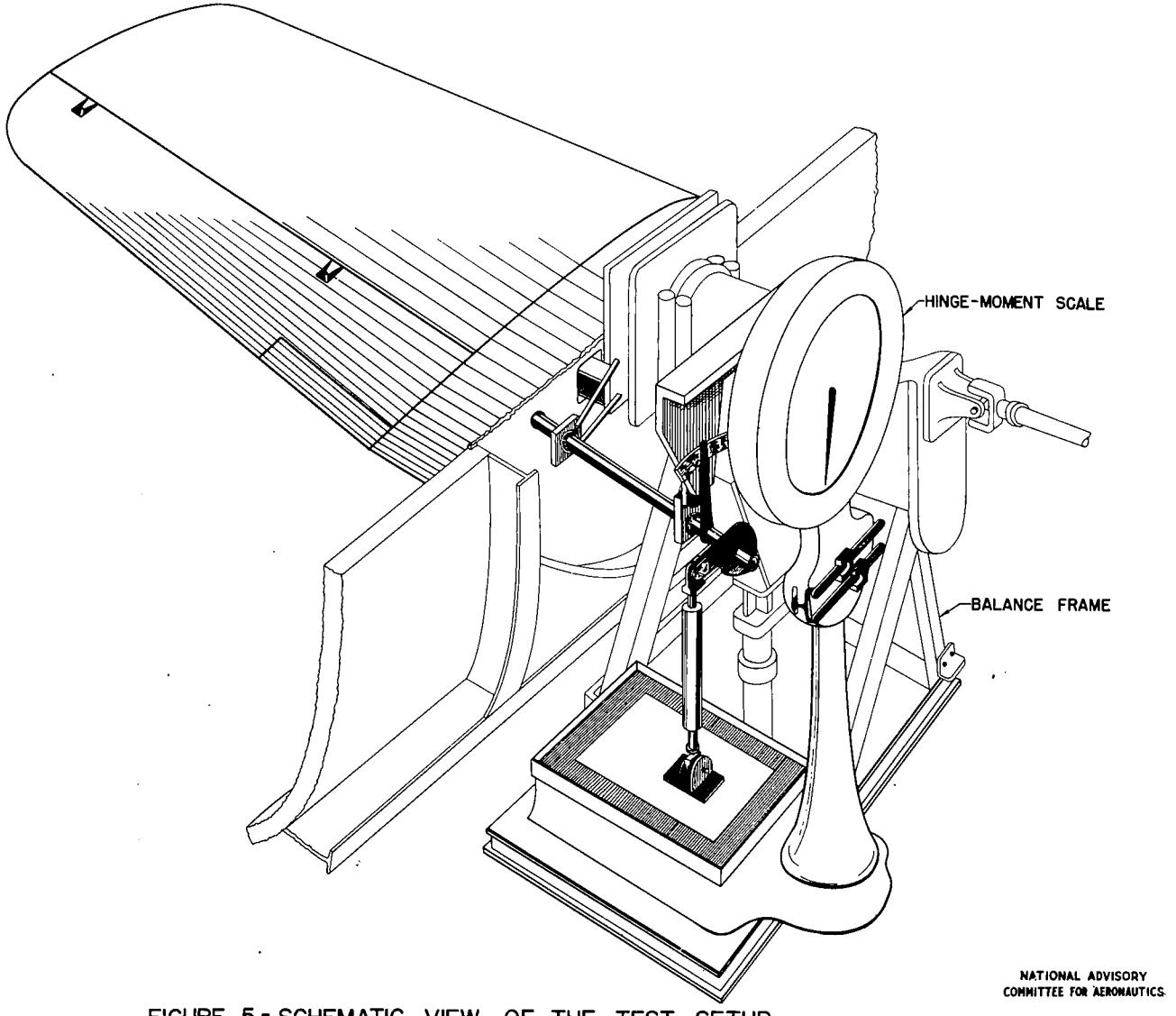

FIGURE 5.- SCHEMATIC VIEW OF THE TEST SETUP.

(a) Upper surface.

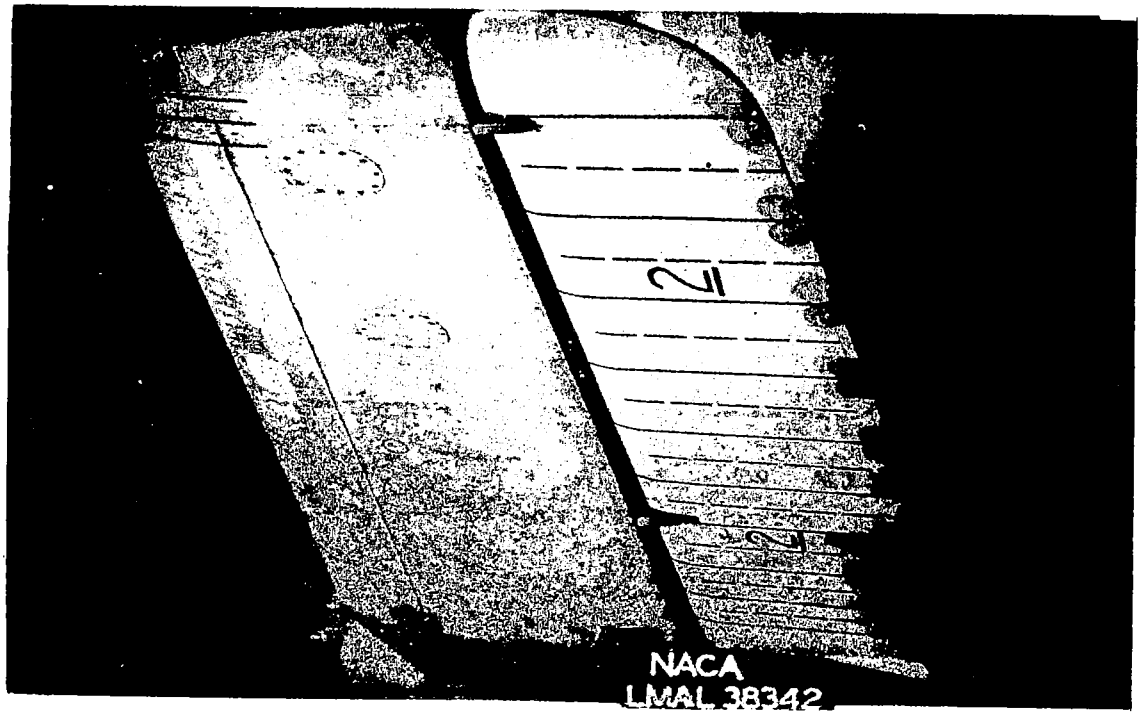

(b) Lower surface.

Figure 6.- Static condition for elevator 2.

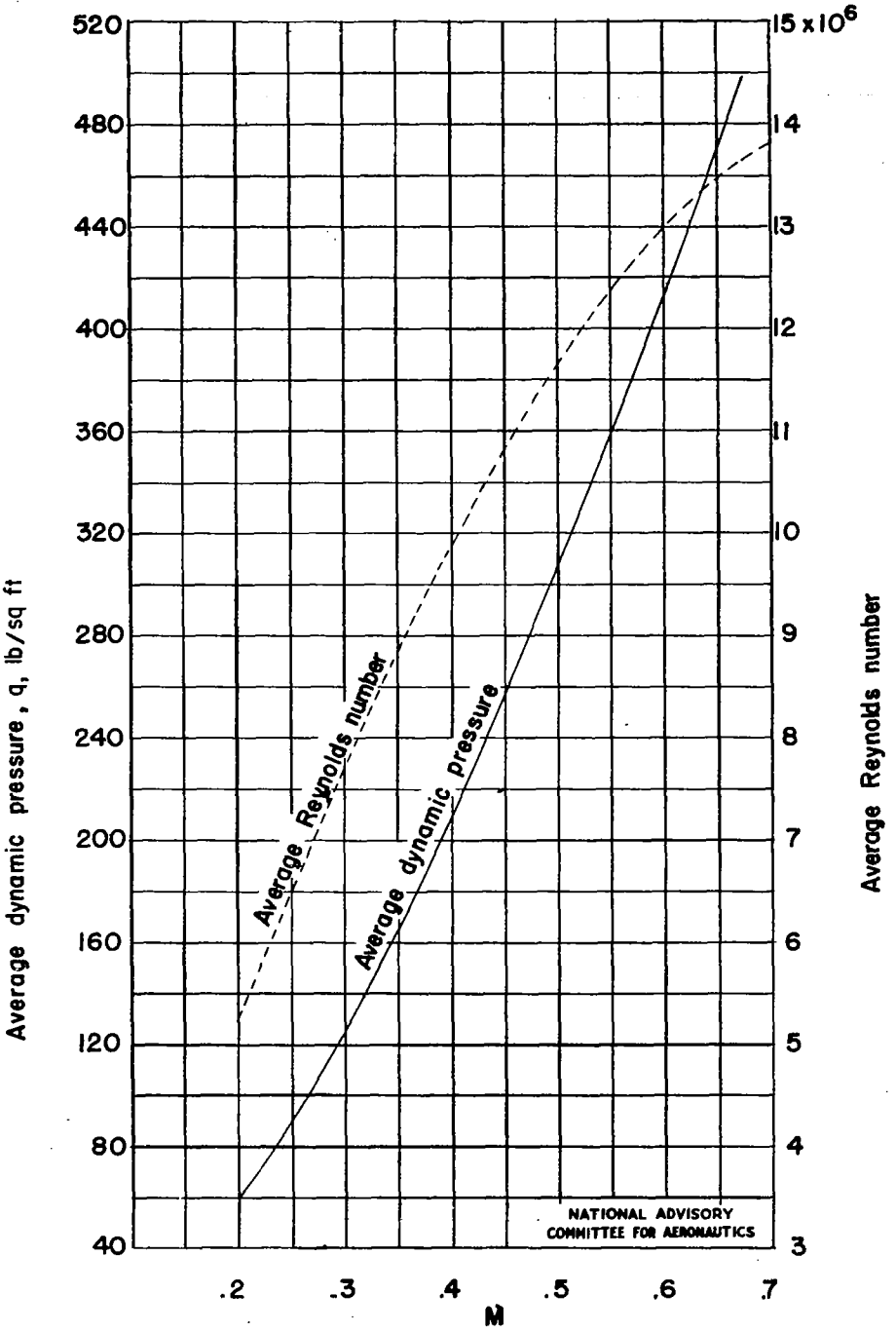

Figure 7.—Variation of the average test Reynolds number and dynamic pressure with test Mach number.

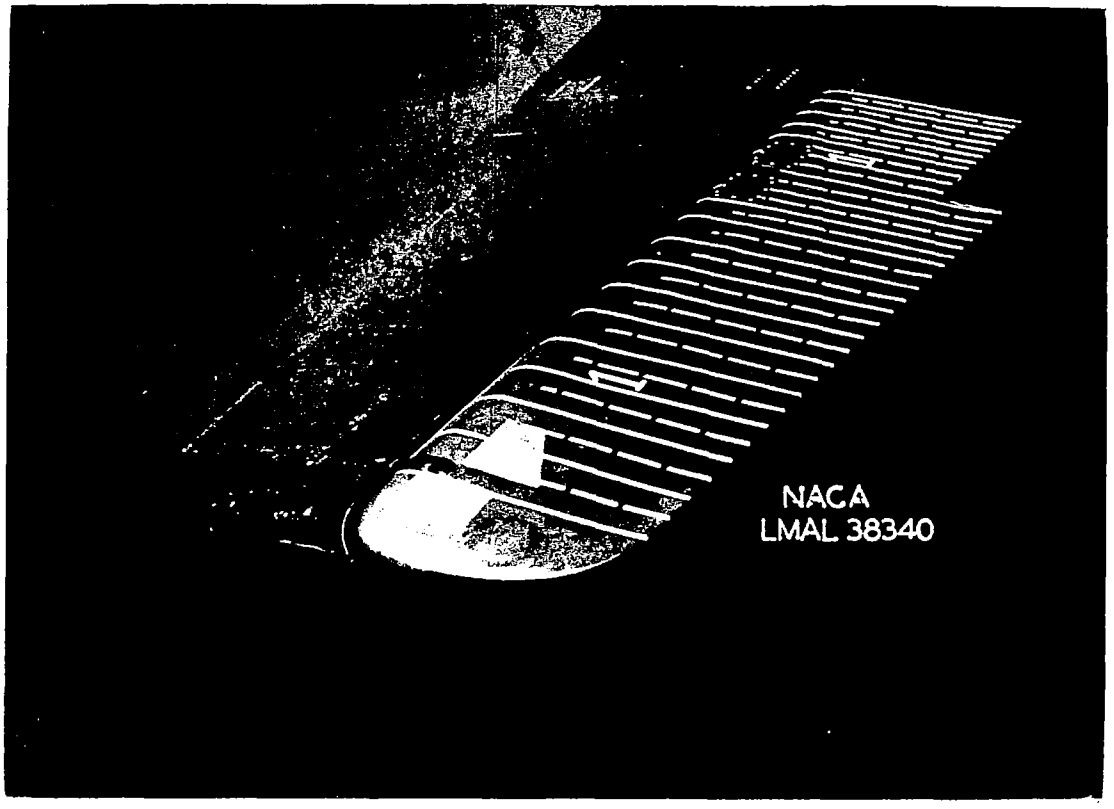

Figure 8.- Fabric deflection of upper surface of elevator 1 (4-inch rib spacing). $M = 0.66$; $\alpha = 0^{\circ}$; $\delta = 4.2^{\circ}$; elevator vents at trailing edge.

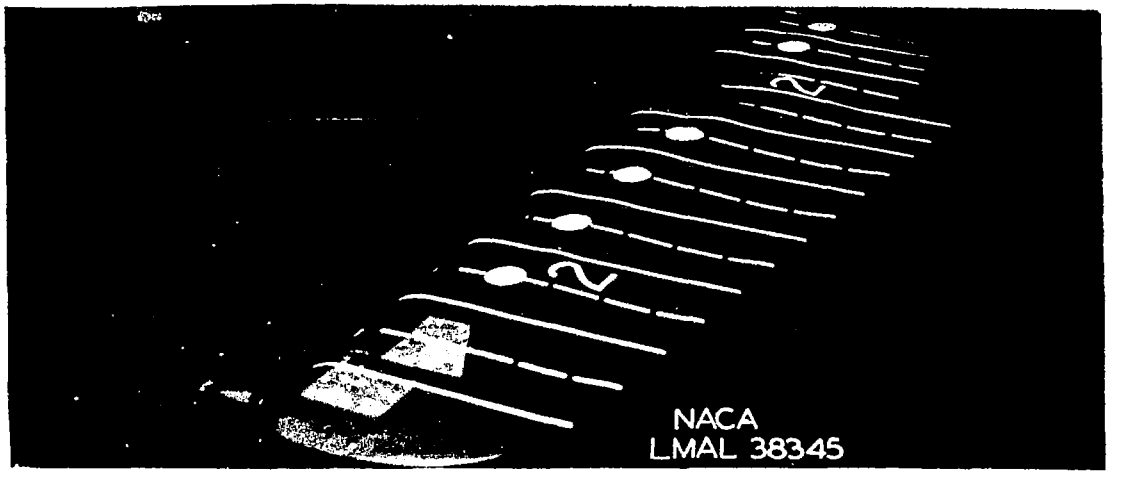

(a) Upper surface.

(b) Lower surface.

Figure 9.- Fabric deflection of elevator 2 (8-inch rib spacing). $M = 0.55$; $\alpha = 0^{\circ}$; $\delta = 3.3^{\circ}$; elevator seal removed; elevator vents at trailing edge.

(a) Upper surface.

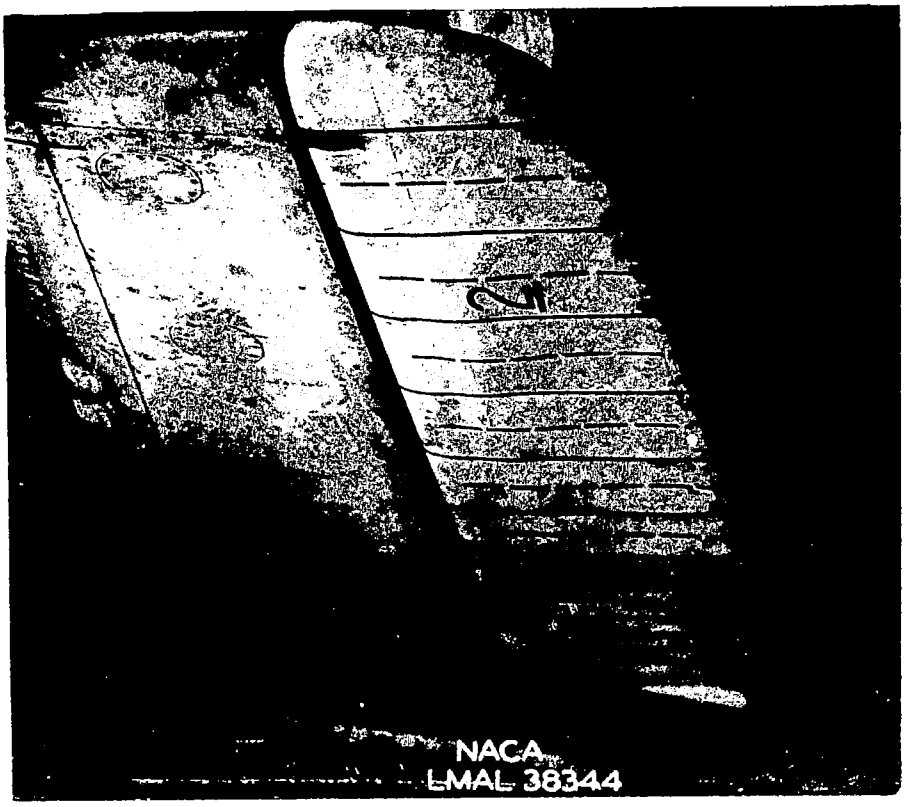

(b) Lower surface.

Figure 10.- Fabric deflection of elevator 2. M = 0.62; $\alpha = 3^{\circ}$; $\delta = -0.7^{\circ}$; elevator vents at trailing edge.

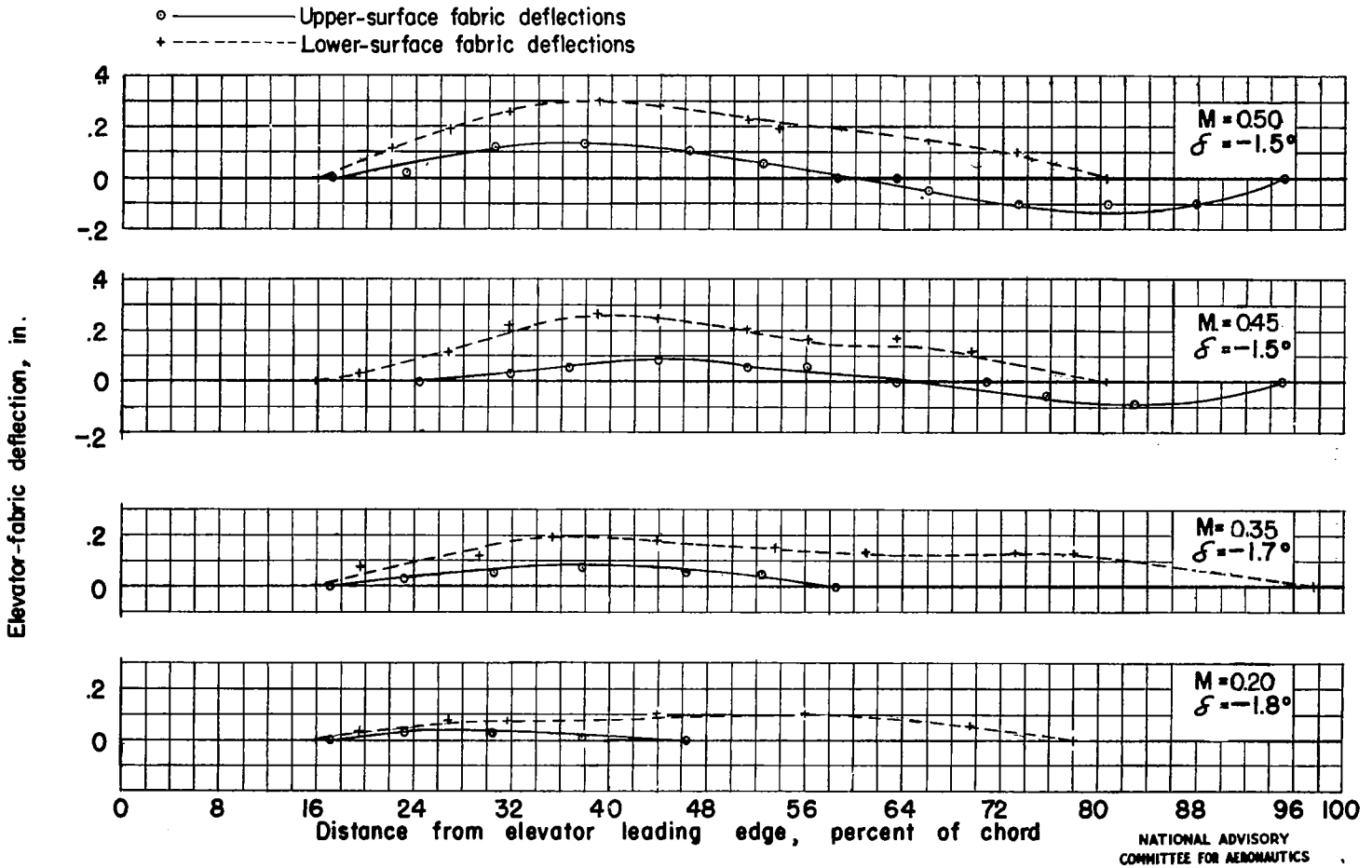

Figure 11 .— The variation of the fabric deflection along the chord of elevator 2 at the 77.1-inch station for various Mach numbers, $\alpha = 0°$; vents on lower surface 1 inch from trailing edge. (Positive deflections denote fabric bulge and negative deflections denote fabric depression.)

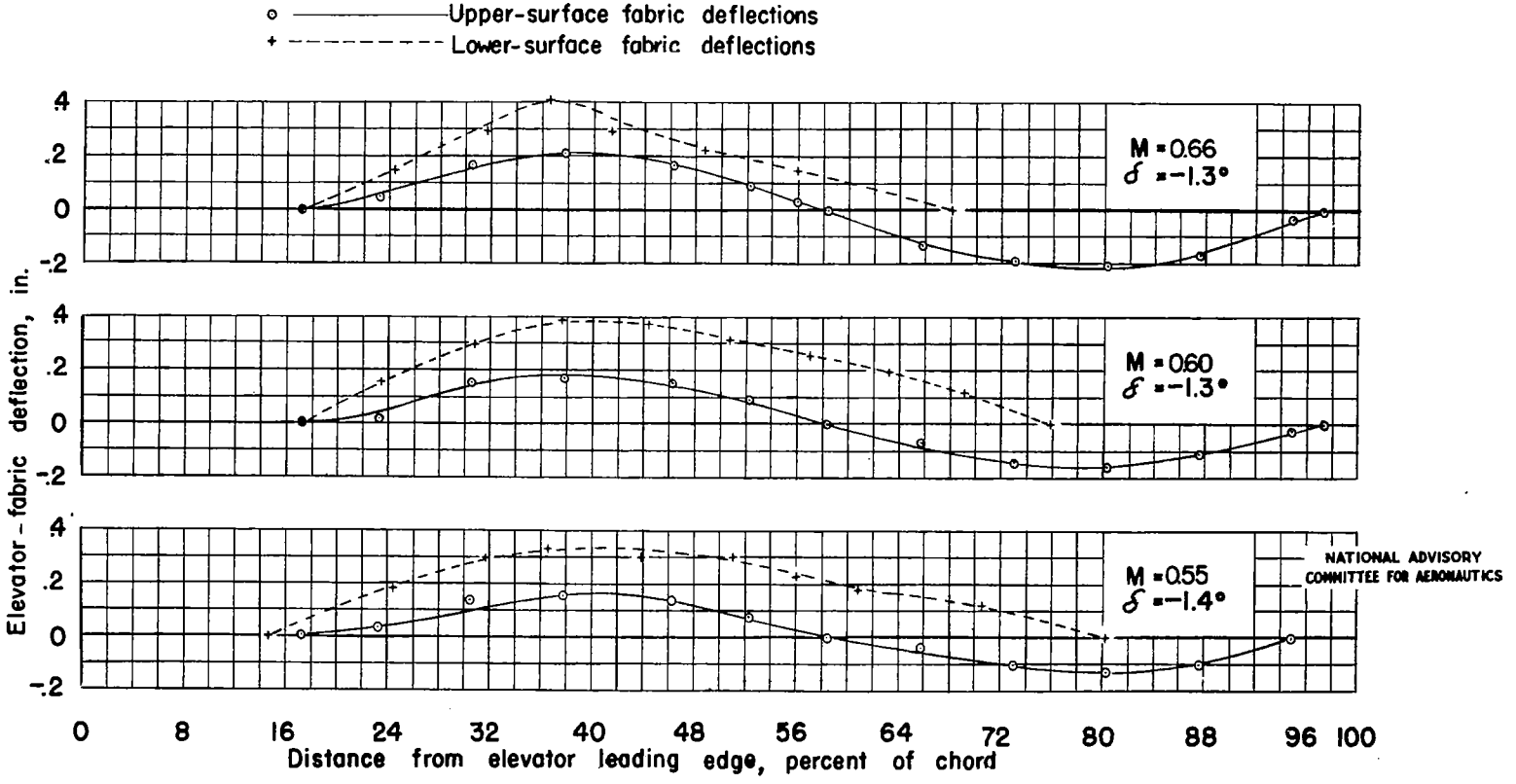

Figure 11 .— Concluded.

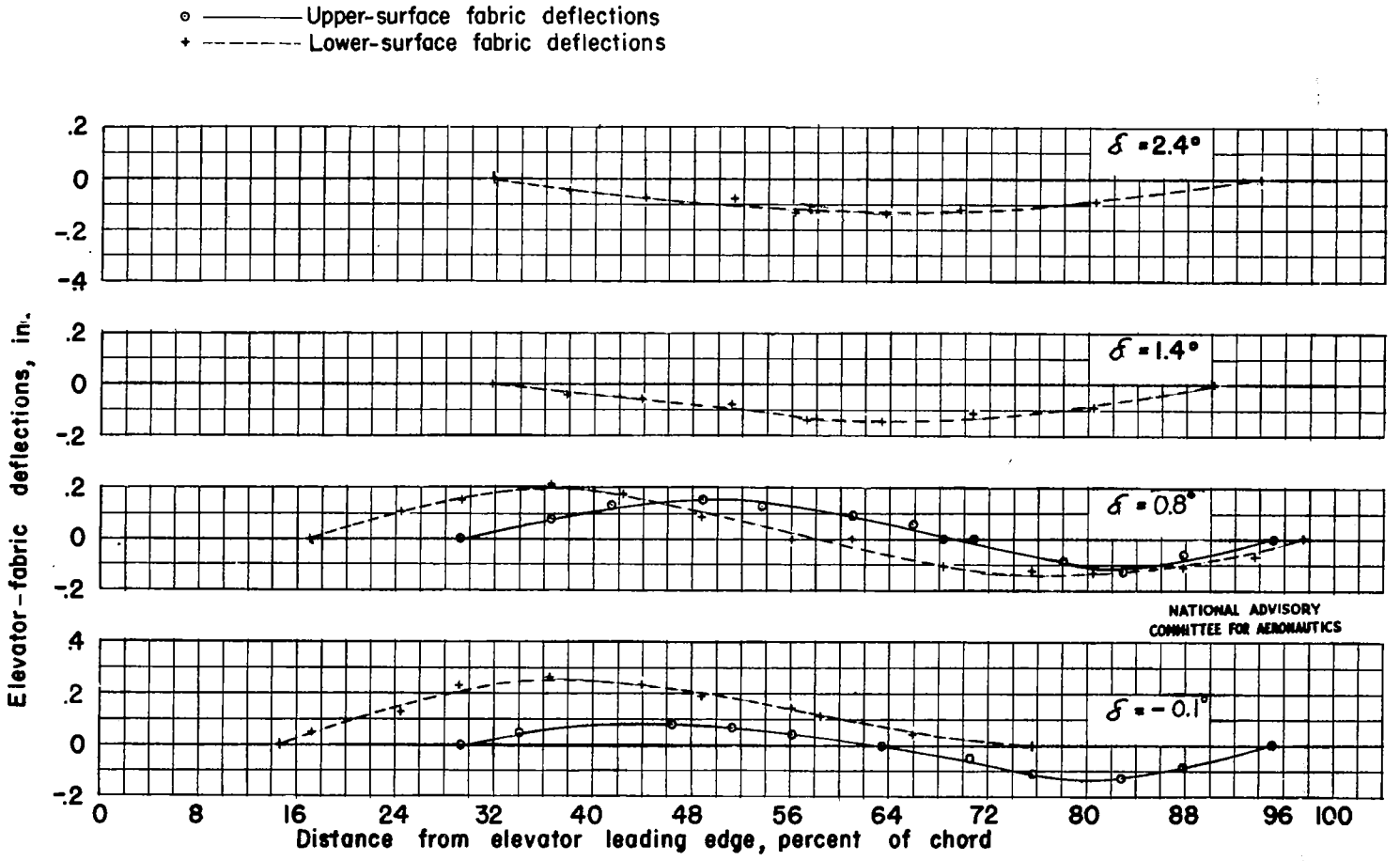

Figure 12 .— The variation of the fabric deflection along the chord of elevator 2 at 77.1-inch station for various elevator angles. $\alpha = 0°$; $M = 0.55$; vents on lower surface 1 inch from trailing edge. (Positive deflections denote fabric bulge and negative deflections denote fabric depression.)

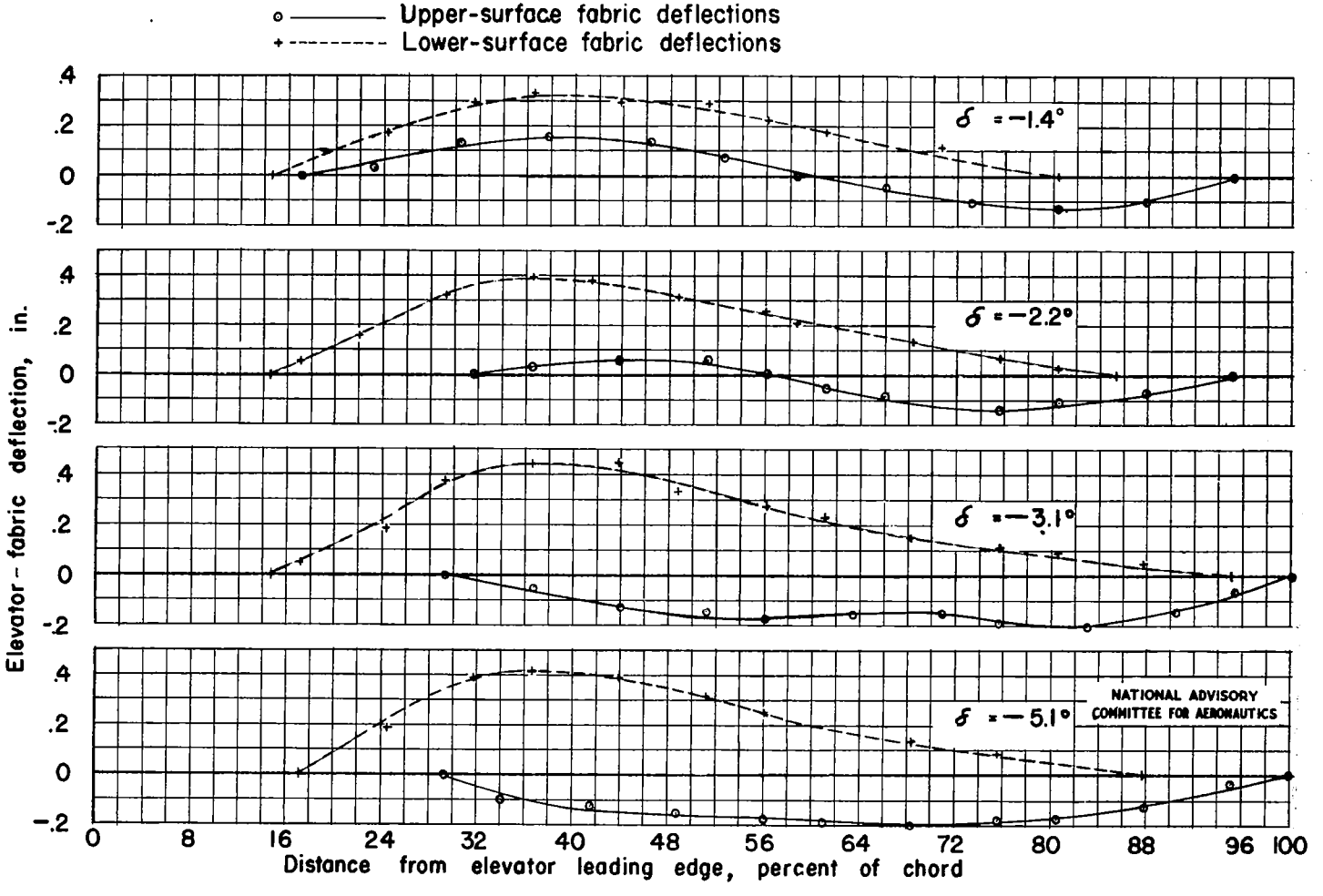

Figure 12 — Concluded.

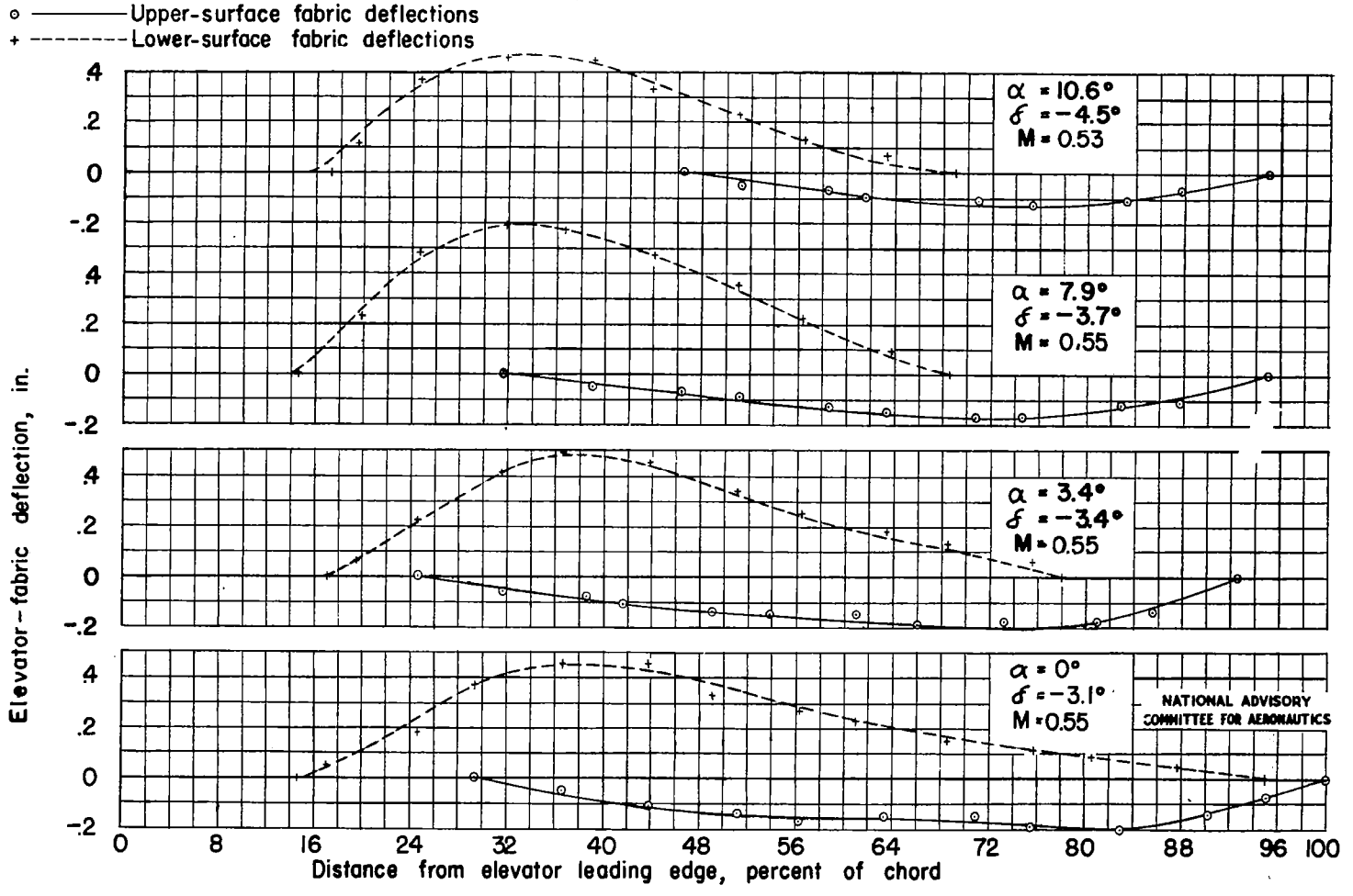

Figure 13.— The variation of the fabric deflection along the chord of elevator 2 at 77.1-inch station for various stabilizer angles. Vents on lower surface 1 inch from trailing edge. (Positive deflections denote fabric bulge and negative deflections denote fabric depression.)

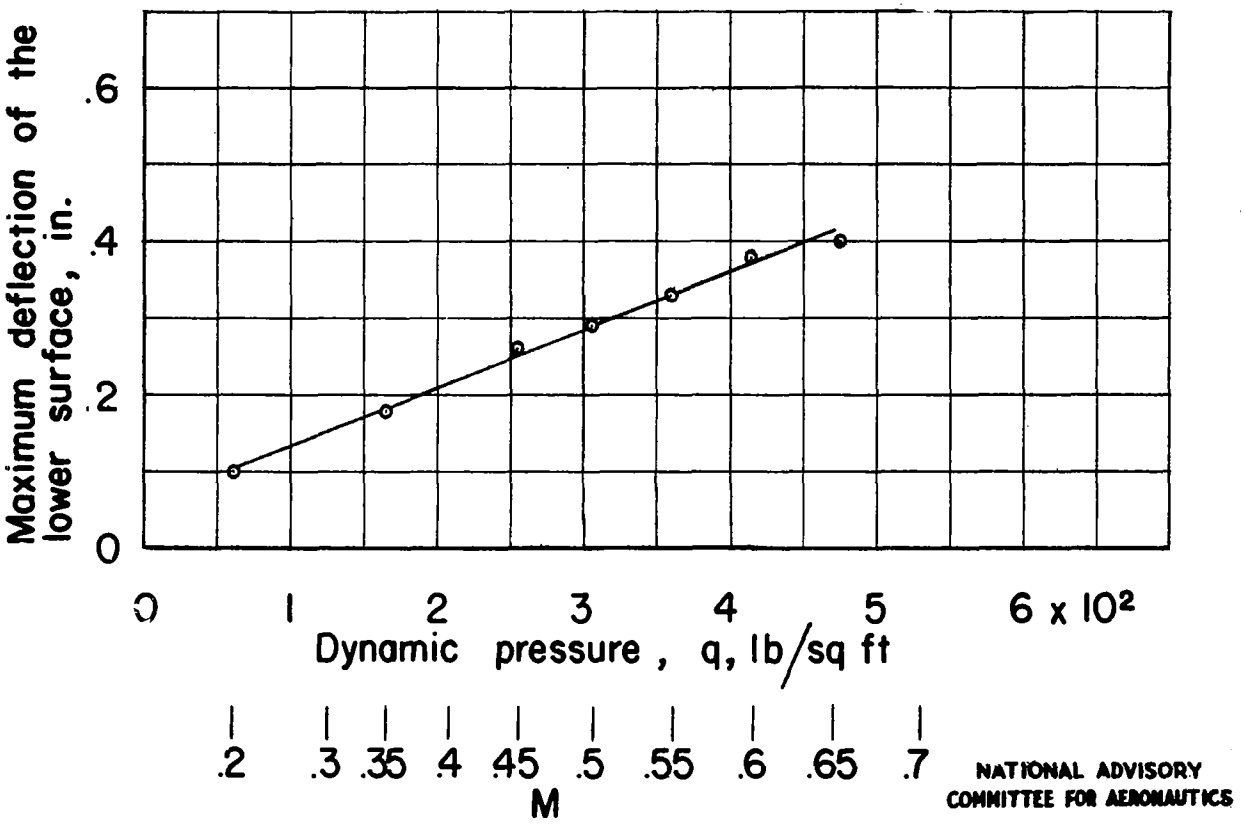

Figure 14 .— Effect of speed on elevator-fabric deflection.

Elevator 2 ; $\alpha = 0°$; $\delta \approx -1.5$.

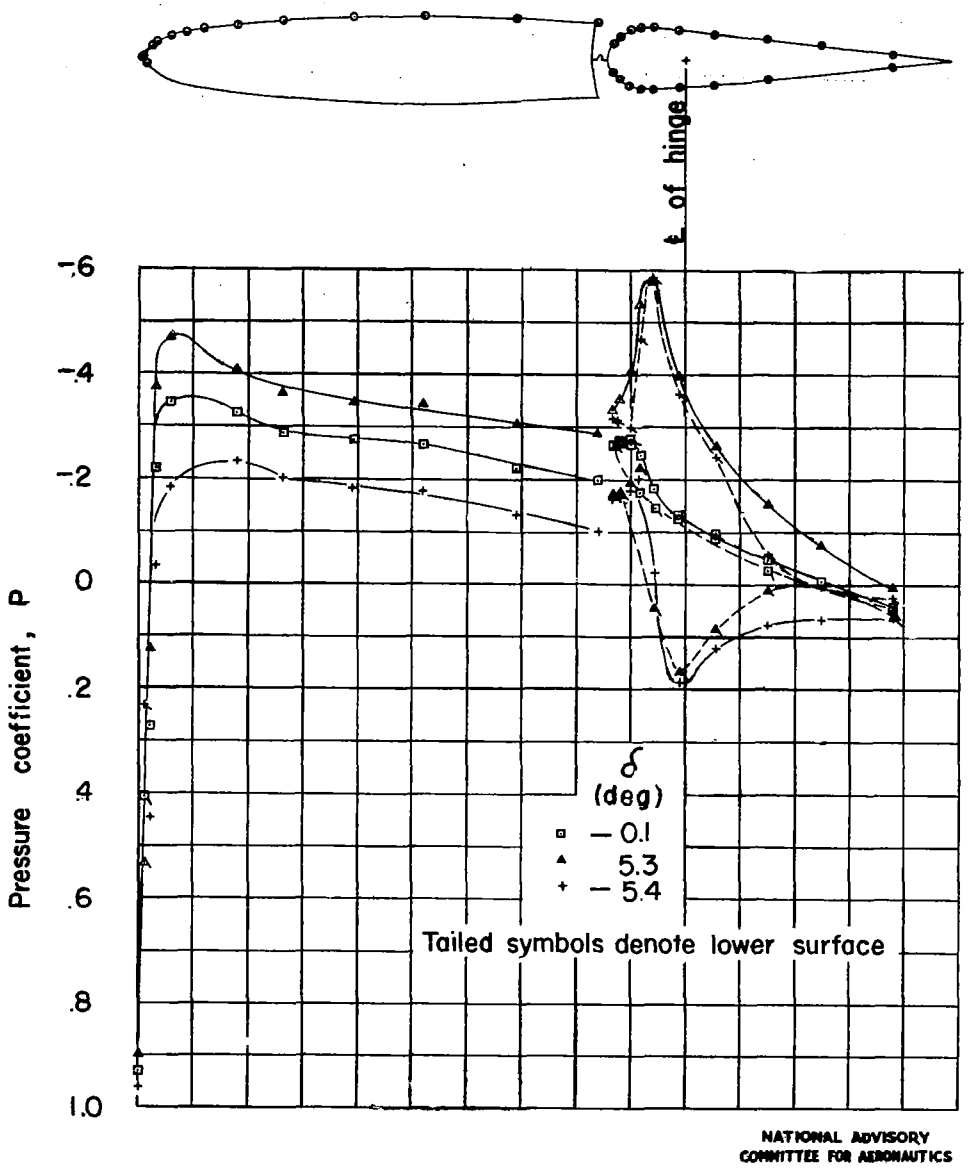

Figure 15 .— Pressure distribution of elevator 3 for three elevator positions. $\alpha = 0°$; $M = 0.20$; gap sealed ; 33-inch station.

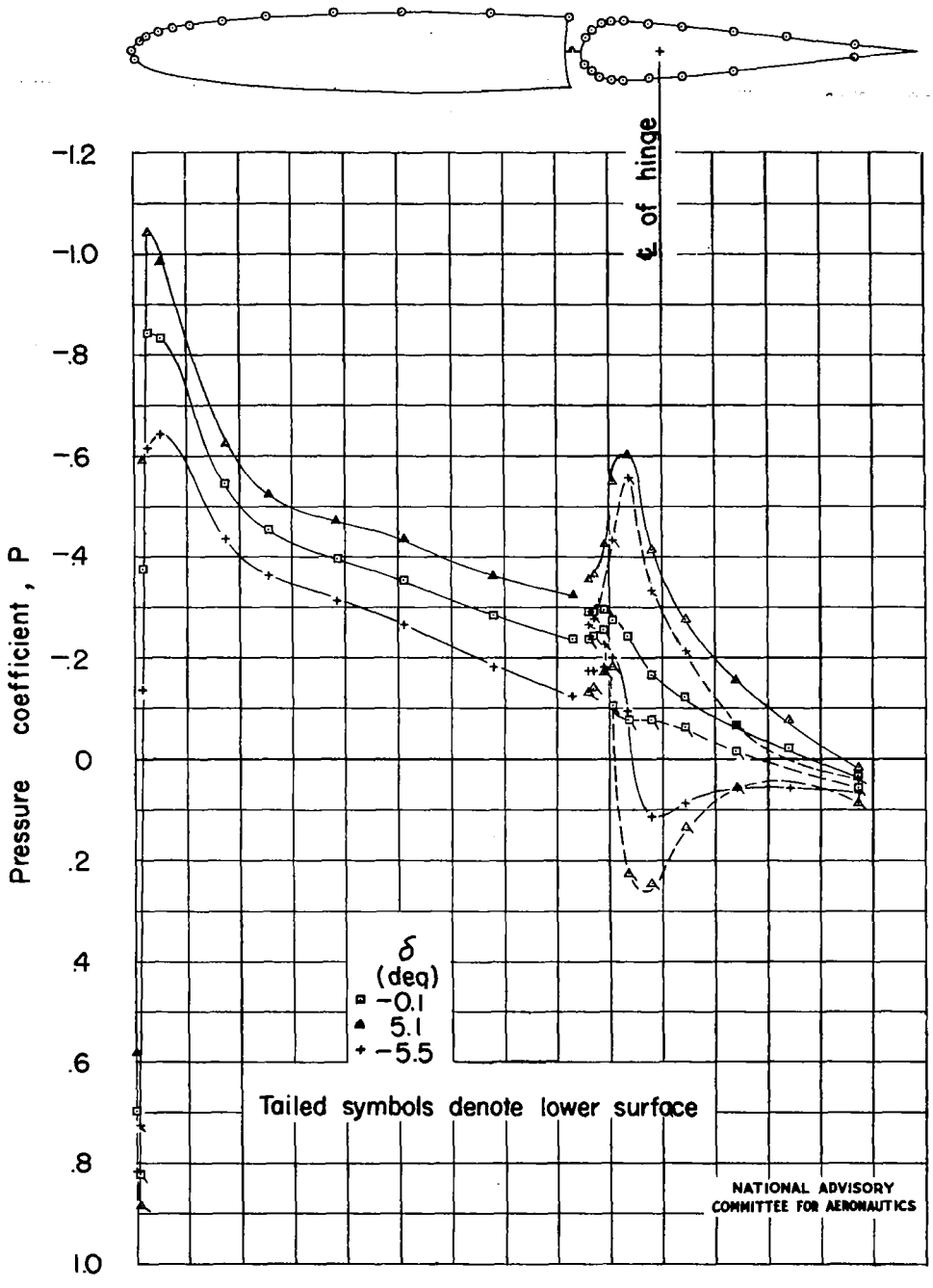

Figure 16.—Pressure distribution of elevator 3 for three elevator positions. $\alpha = 3°$; gap sealed; 33-inch station; $M = 0.20$.

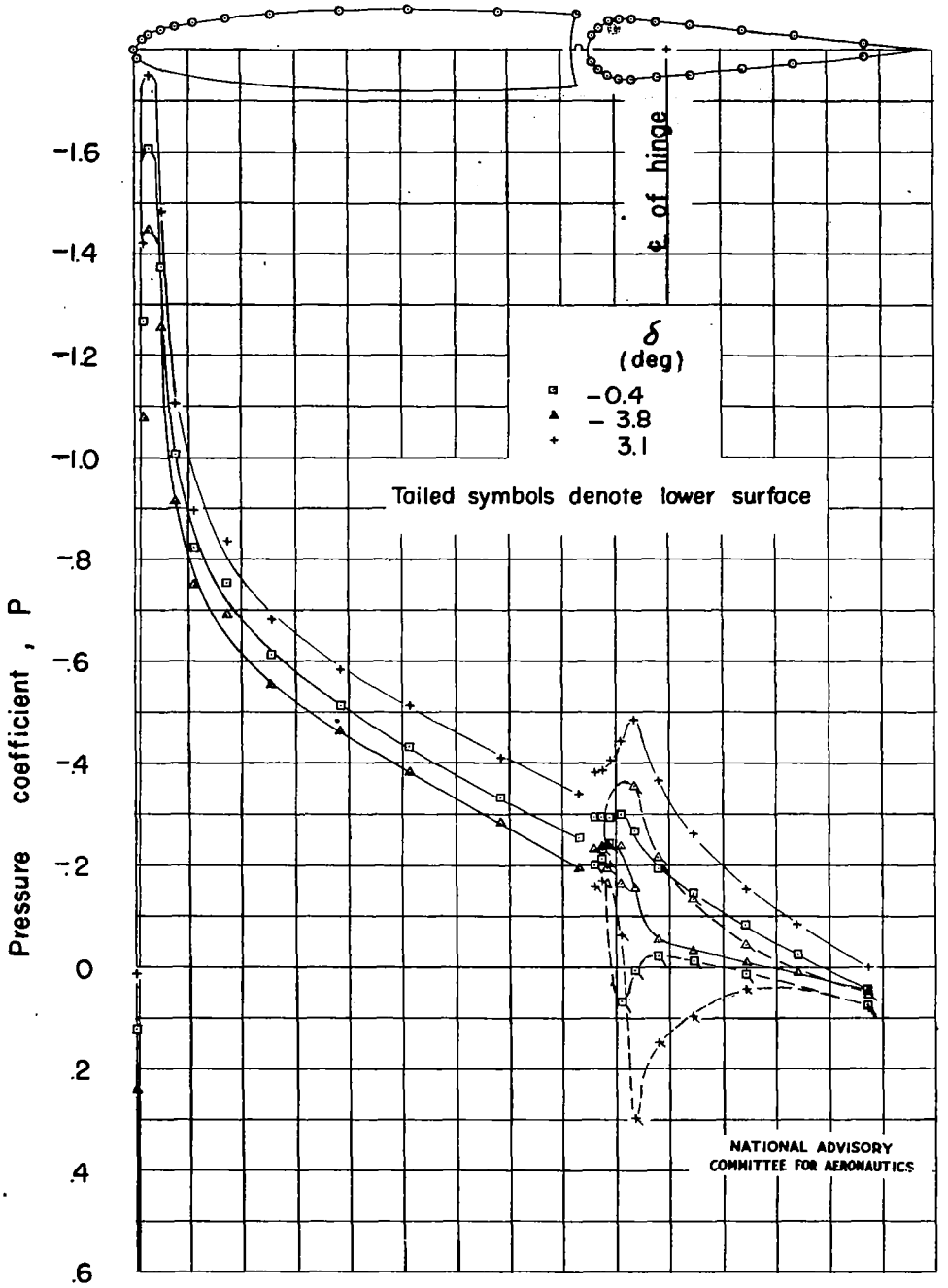

Figure 17.—Pressure distribution of elevator 3 for three elevator positions. $\alpha = 6°$; M = 0.20; gap sealed; 33-inch station.

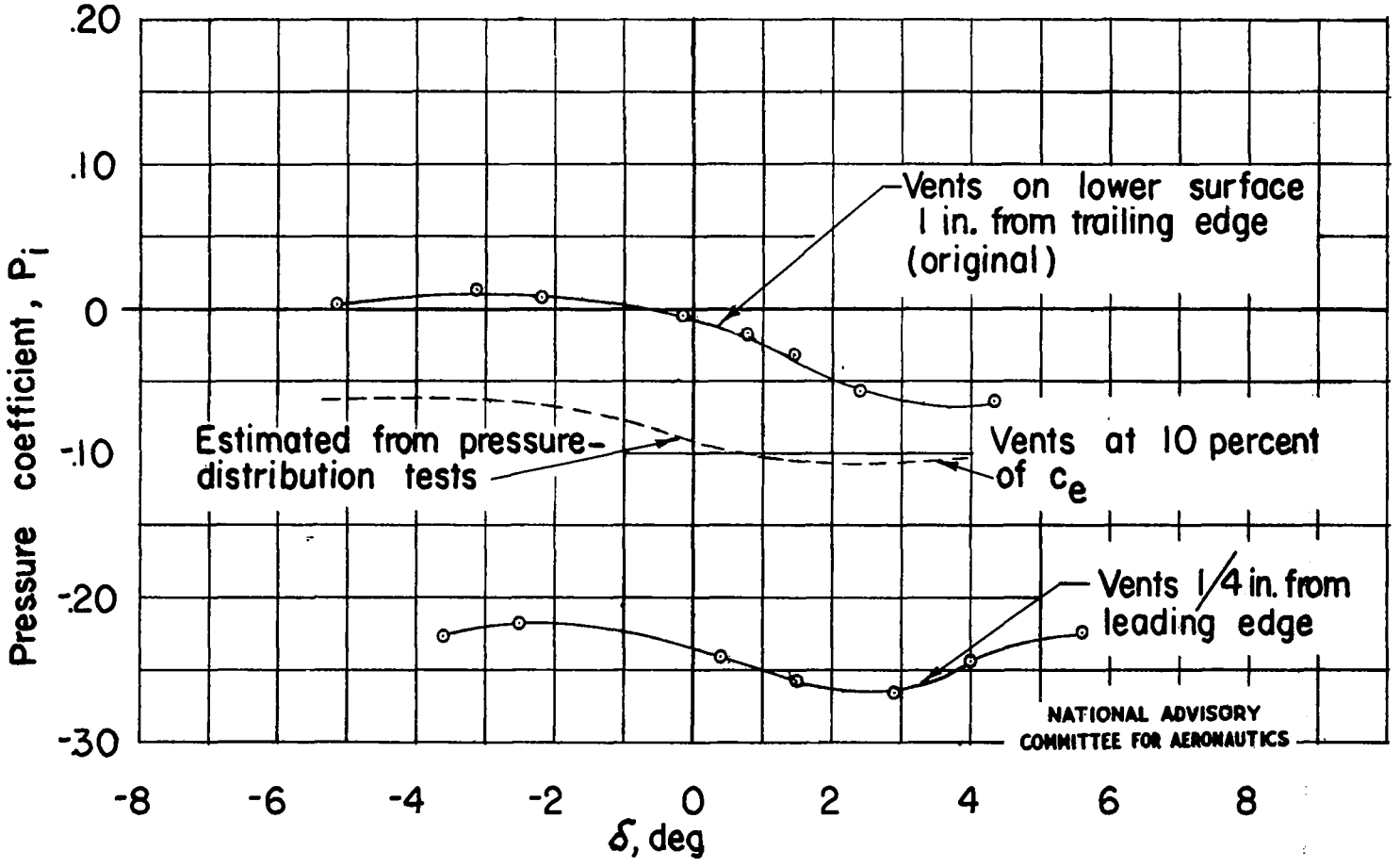

Figure 18 .—Variation of the elevator internal-pressure coefficient with elevator position. α = 0°, M = 0.20; elevator 2.

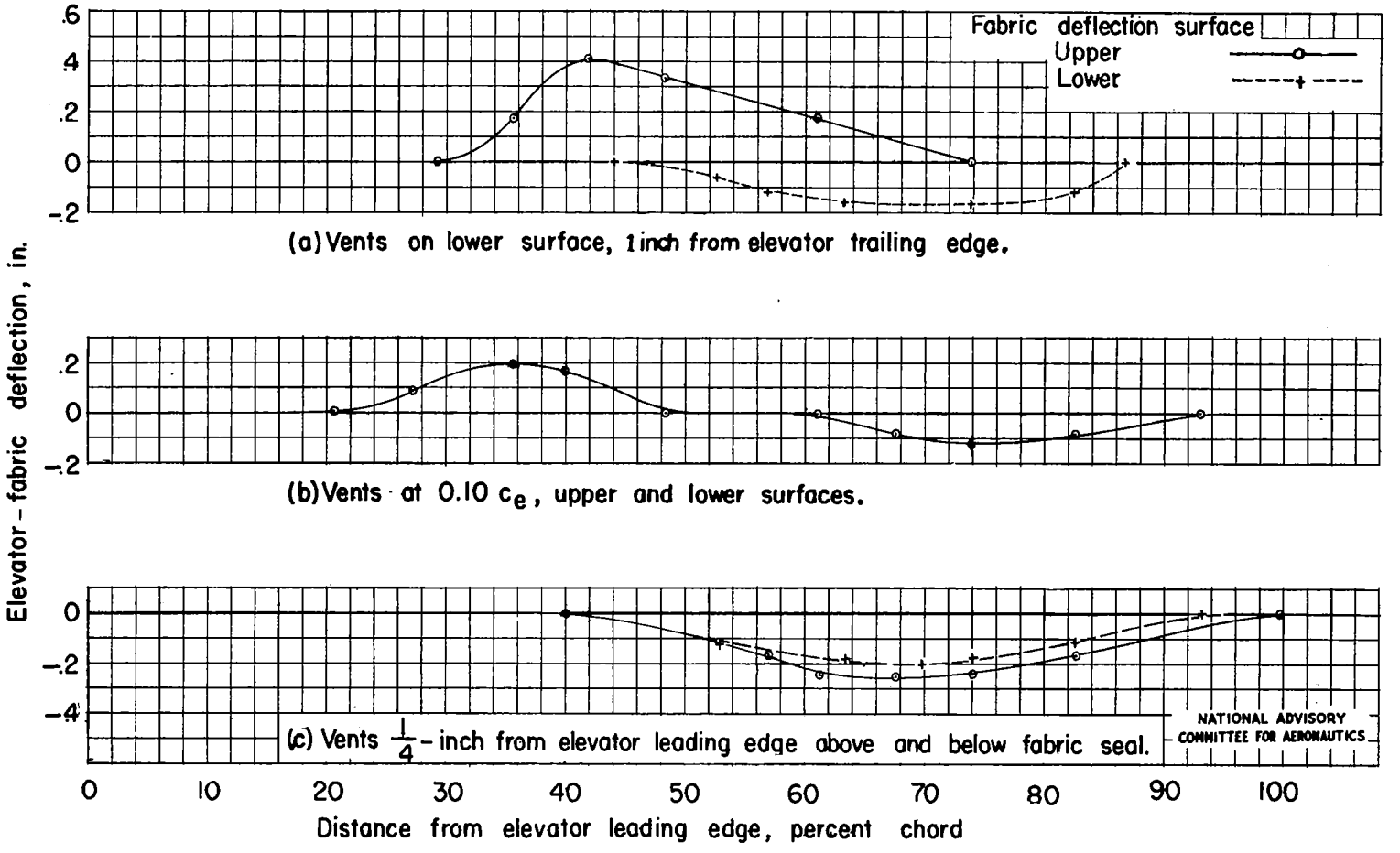

Figure 19.— The variation of the fabric deflection along the chord of elevator 2 at 51.5-inch station for three vent configurations. $\alpha = 0°$; $\delta = 4°$; $M = 0.55$. (Positive deflections denote fabric bulge and negative deflections denote fabric depression.)

(a) Upper surface.

(b) Lower surface.

Figure 20.- Fabric deflection of elevator 2. M = 0.55; $\alpha = 0^{\circ}$; $\delta = 4^{\circ}$; elevator vents at leading edge.

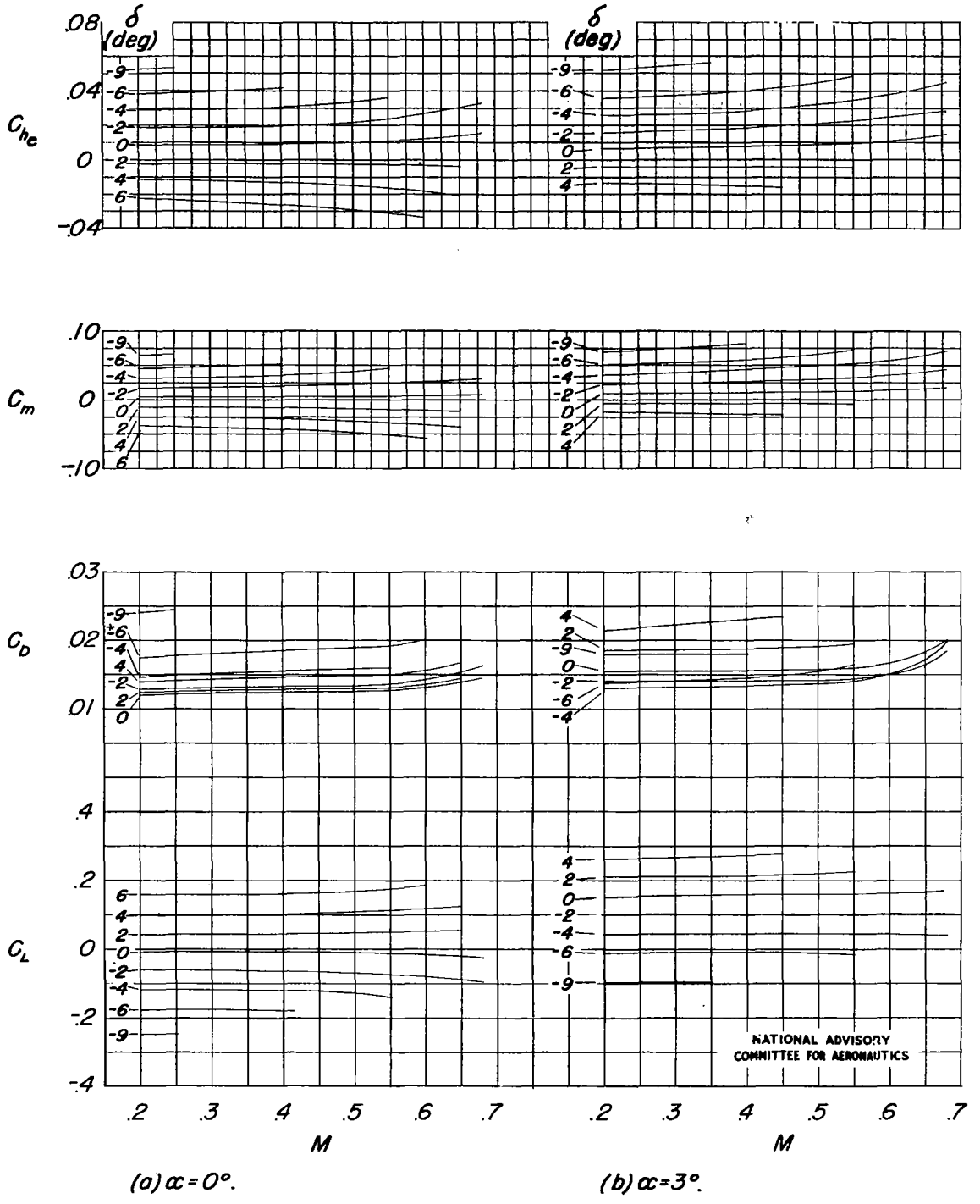

(a) $\alpha = 0°$. (b) $\alpha = 3°$.

Figure 21.—Variation of the aerodynamic characteristics with Mach number for ranges of elevator angle and angle of attack; elevator 1.

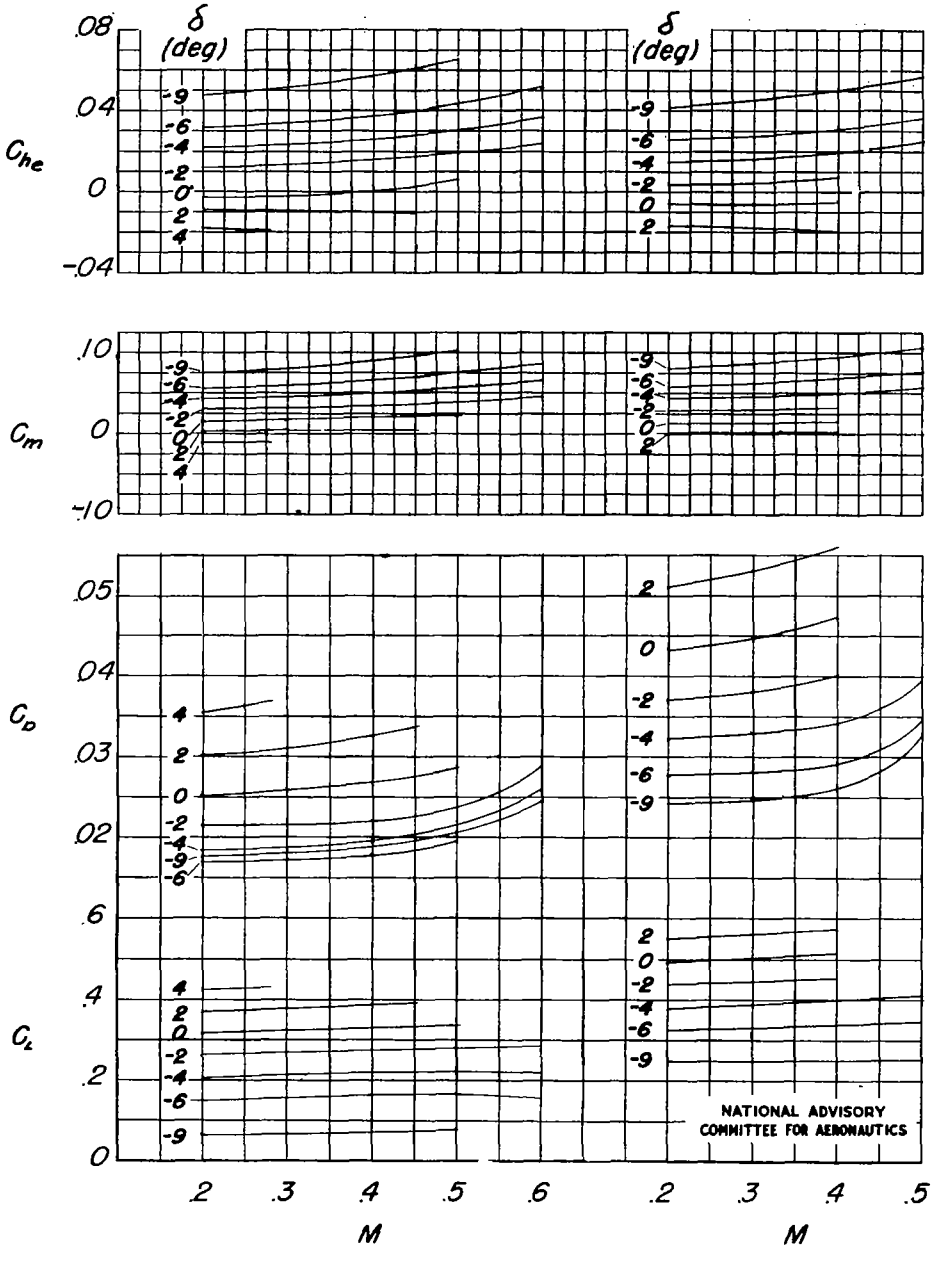

(c) $\alpha = 6°$. (d) $\alpha = 9°$.

Figure 21 .— Concluded.

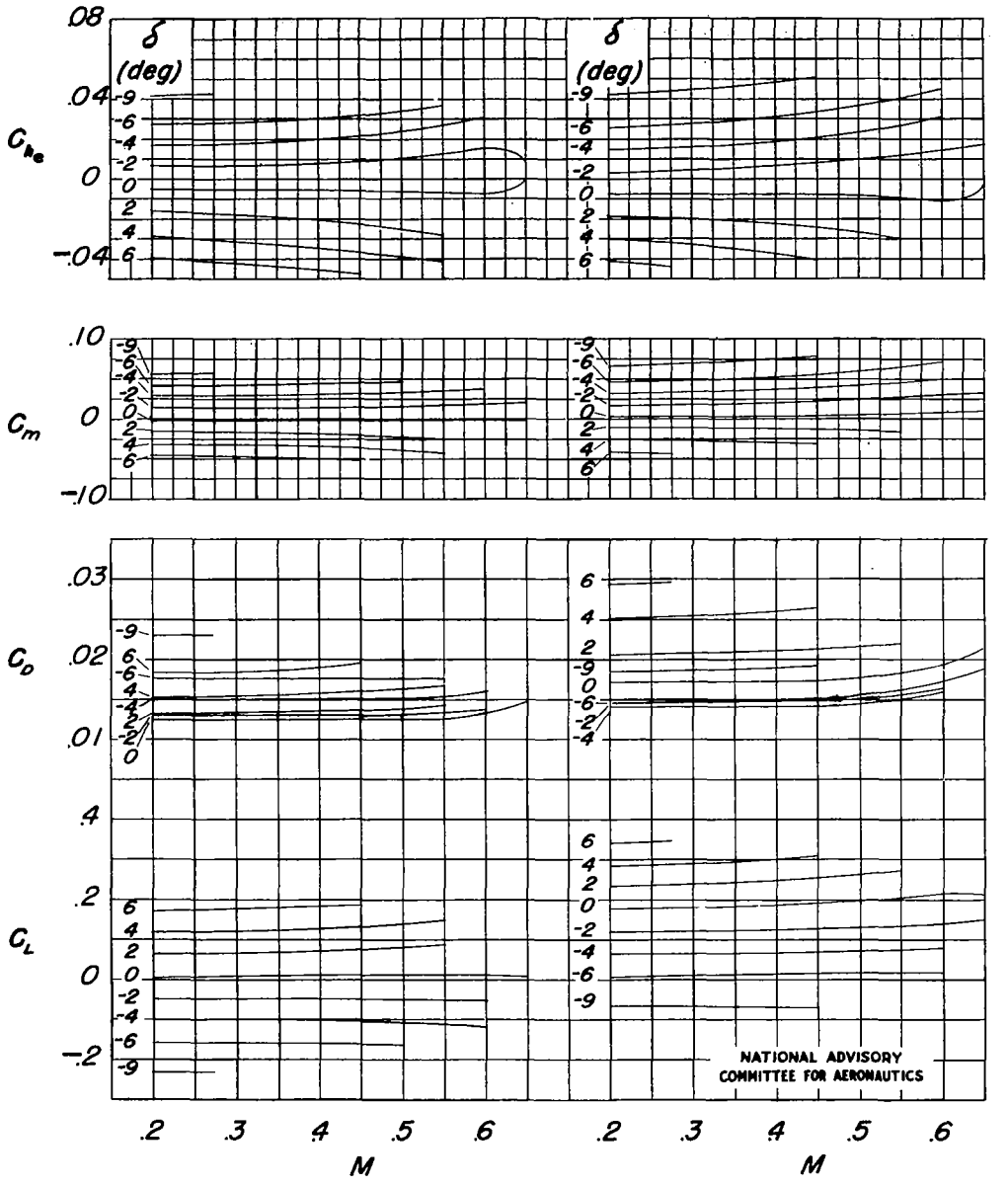

(a) $\alpha = 0°$. (b) $\alpha = 3°$.

Figure 22. – Variation of the aerodynamic characteristics with Mach number for ranges of elevator angle and angle of attack; elevator 2.

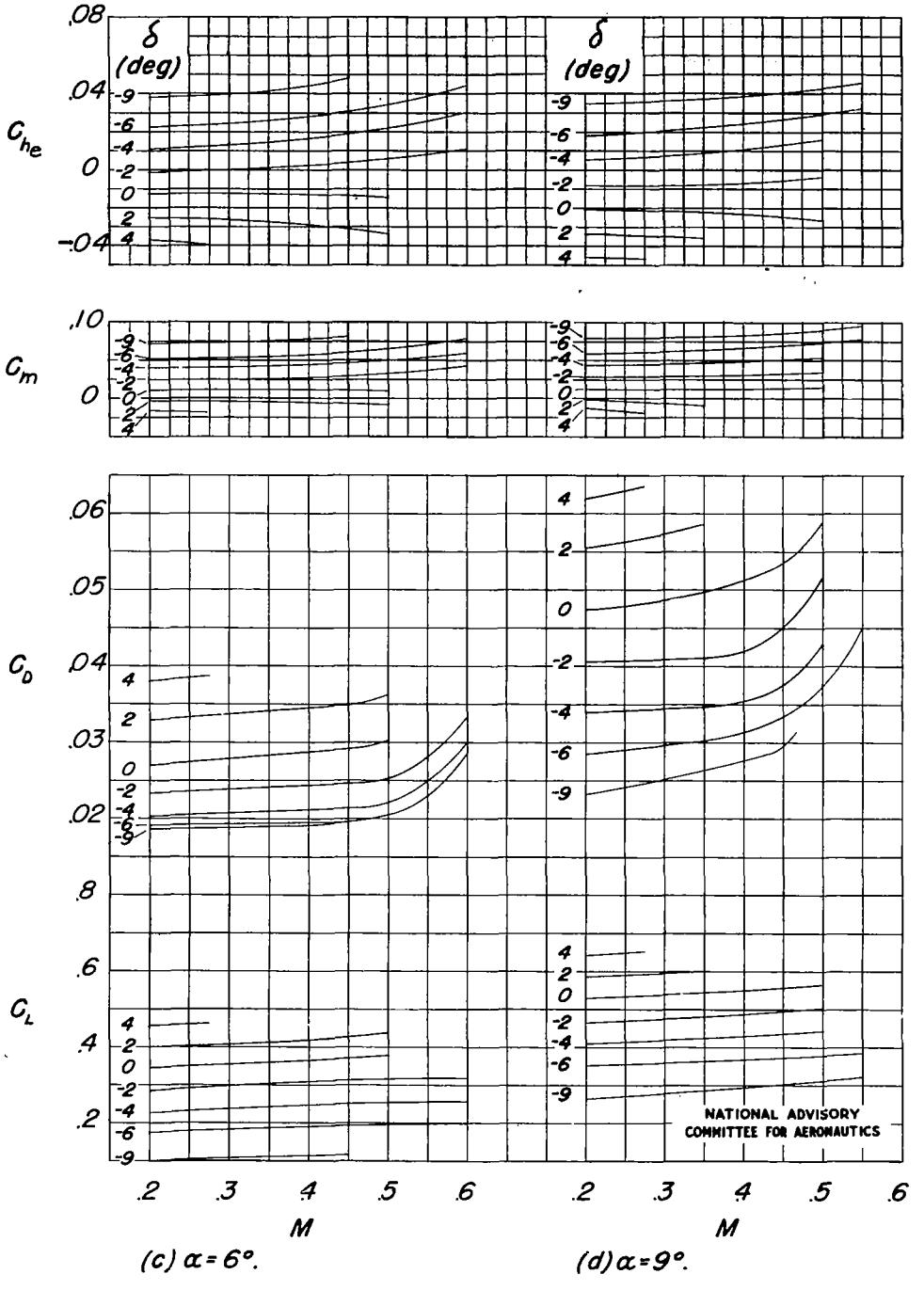

Figure 22 .— Concluded.

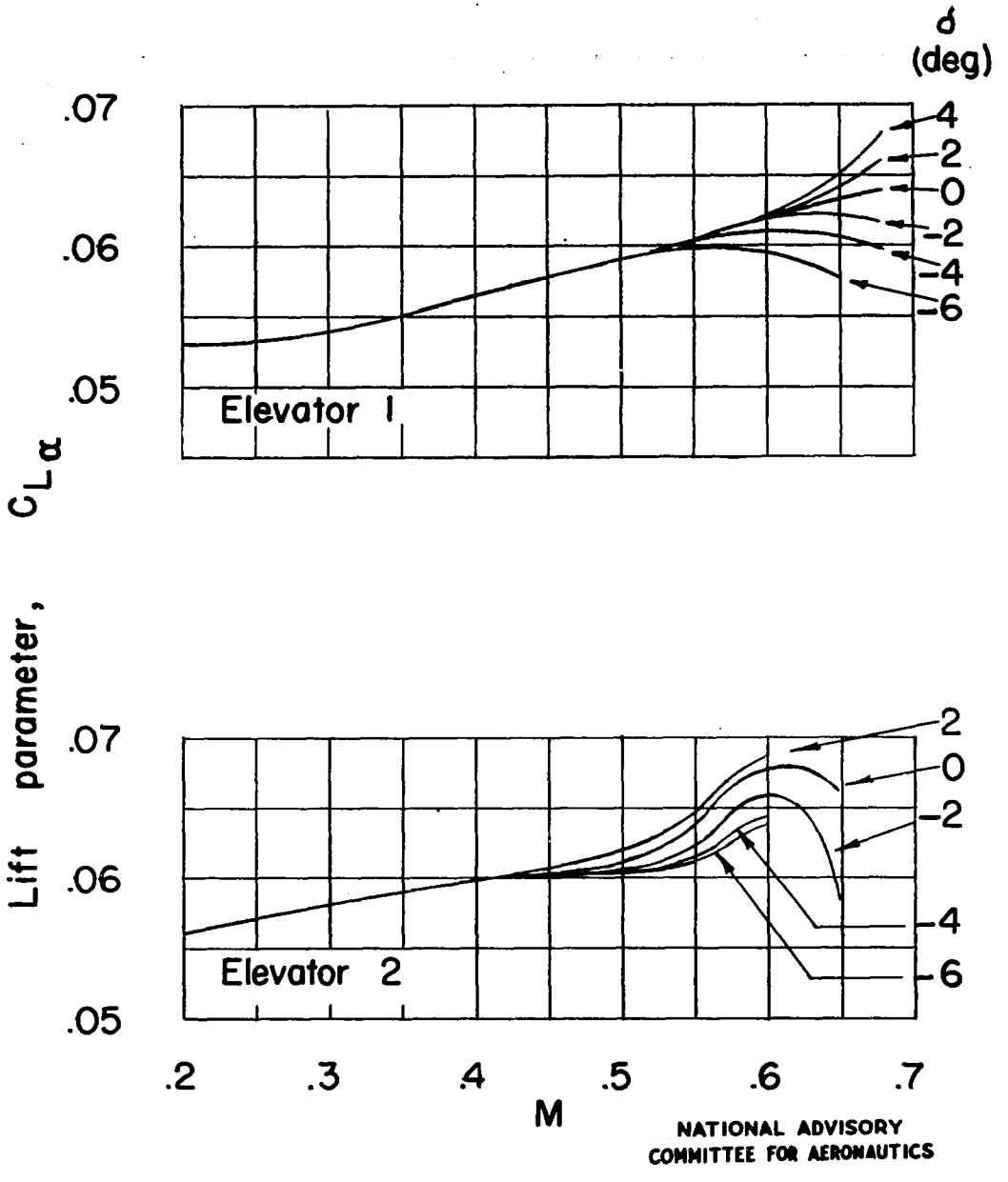

Figure 23.— Variation of the lift parameter $C_{L\alpha}$ with Mach number for elevators 1 and 2.

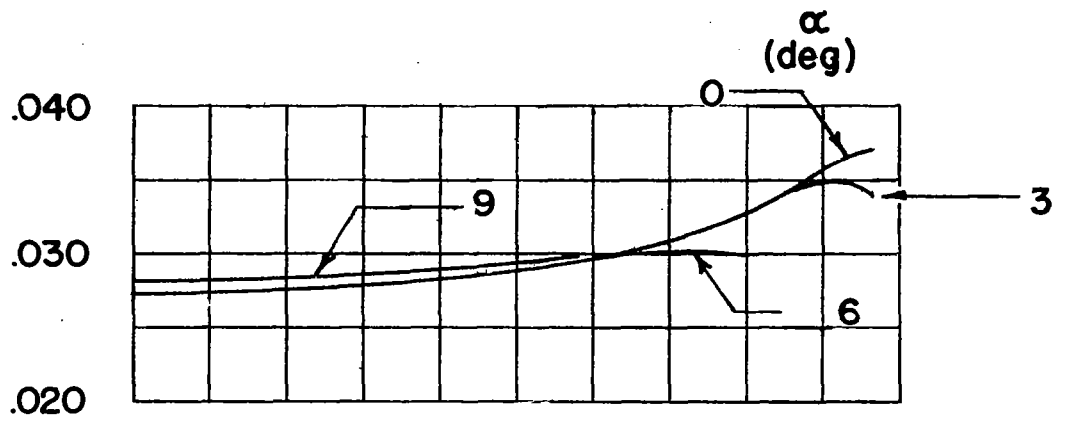

(a) Elevator 1.

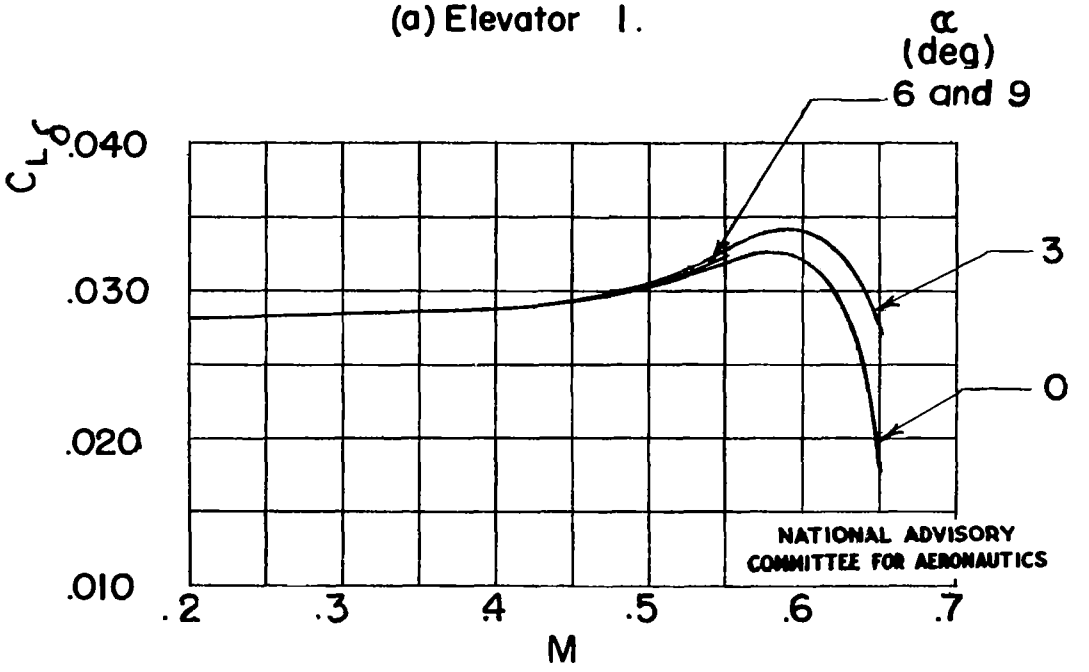

(b) Elevator 2.

Figure 24.—Variation of the lift parameter C_{L_δ} with Mach number for elevators 1 and 2.

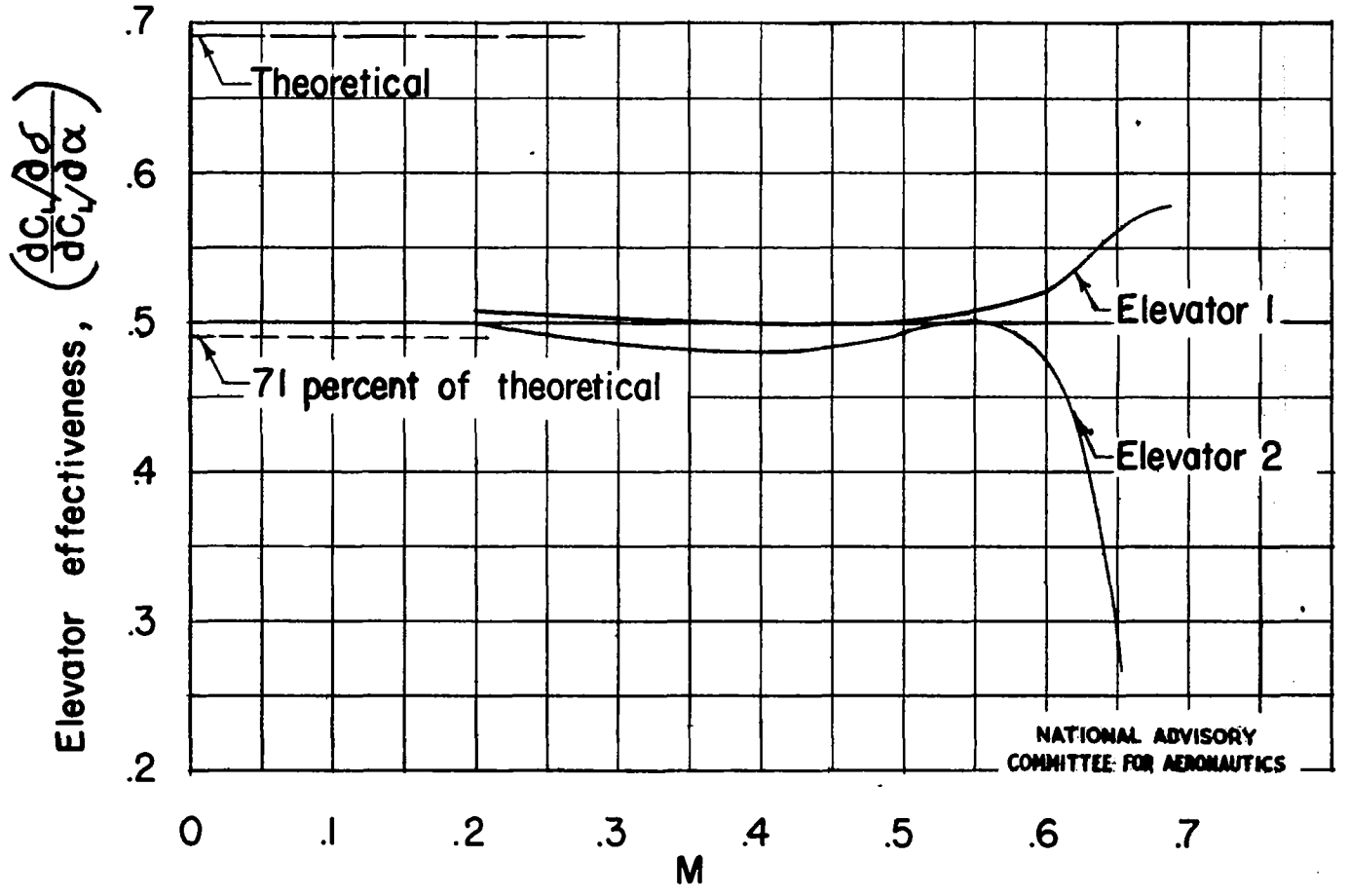

Figure 25 .— Effect of Mach number on elevator effectiveness for elevators 1 and 2; $C_L = 0$.

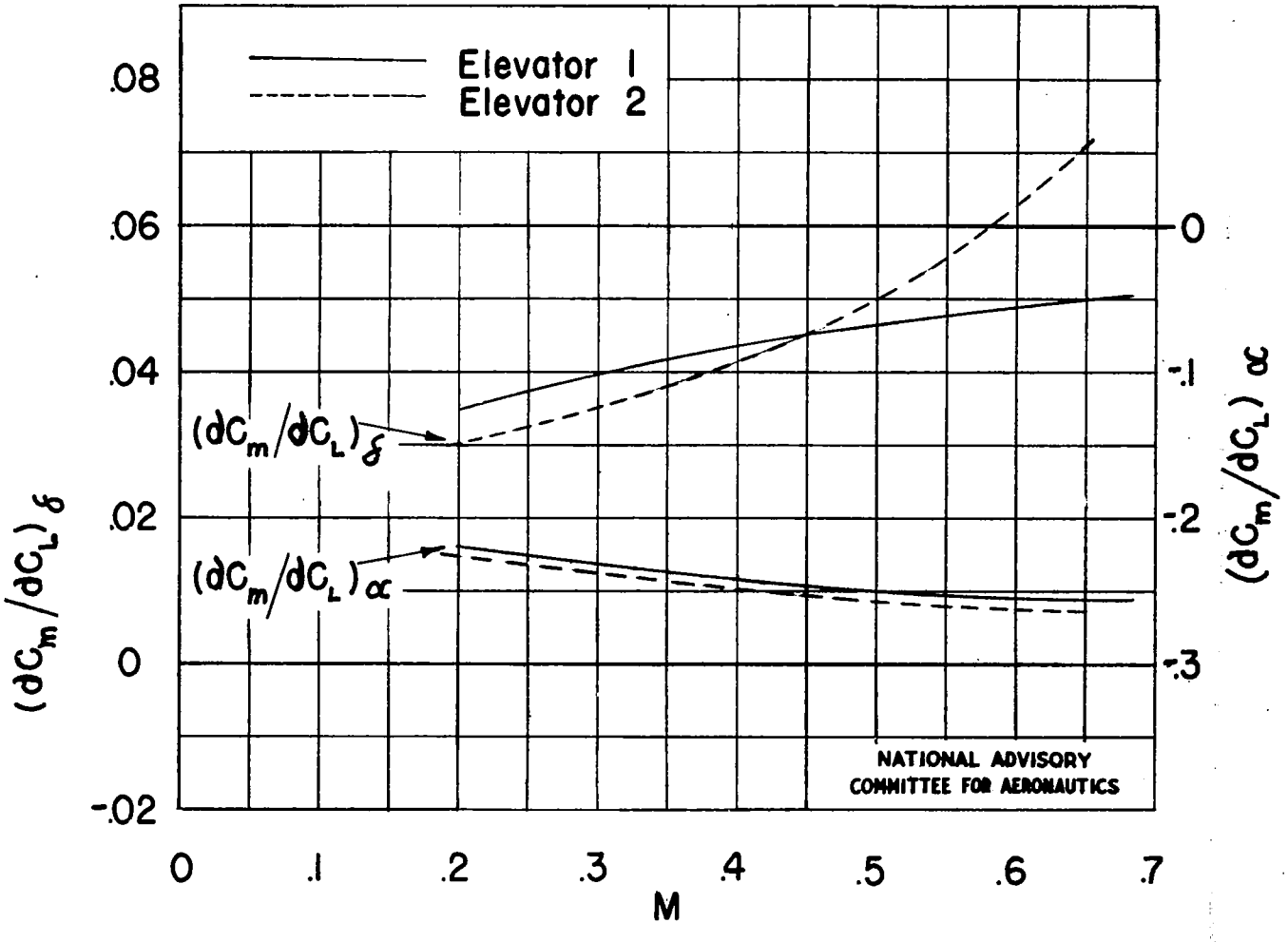

Figure 26.— Comparison of the pitching-moment parameters for elevators 1 and 2.

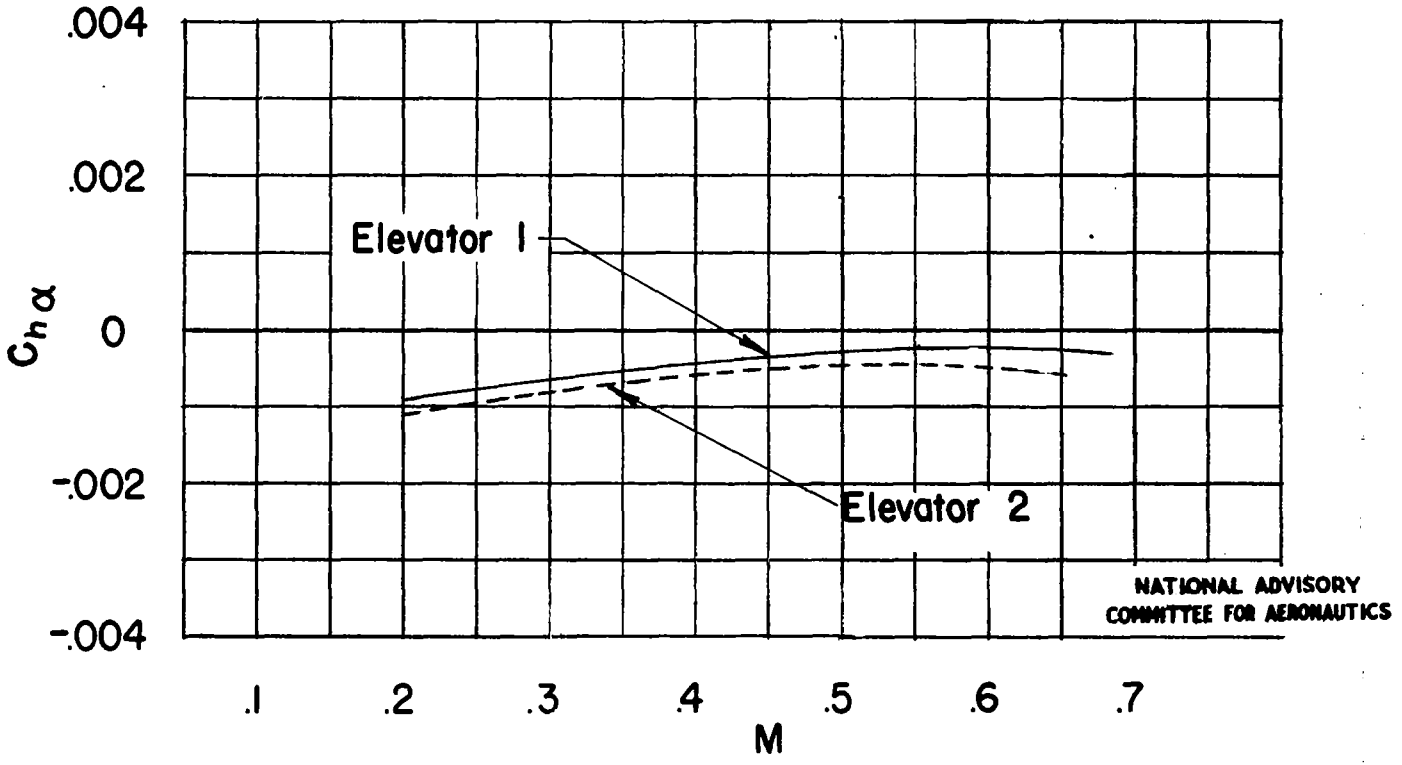

Figure 27 .— A comparison of the change in $C_{h_{\alpha_c}}$ with Mach number for elevators 1 and 2; $\delta_e = 0°$.

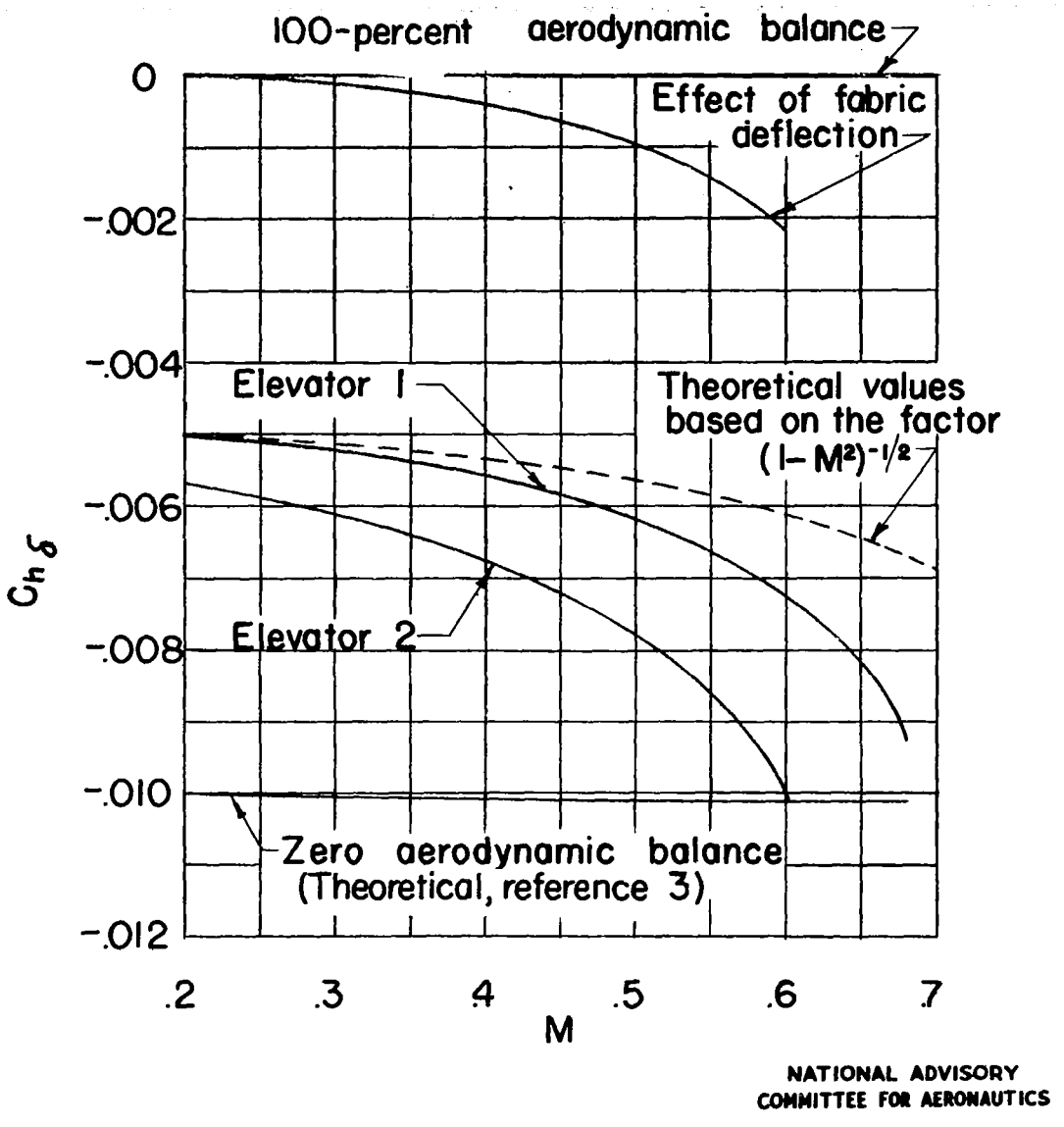

Figure 28 .—Variation of the hinge-moment parameter C_{h_δ} with Mach number for elevators 1 and 2 ; $\alpha = 0°$ or $3°$.

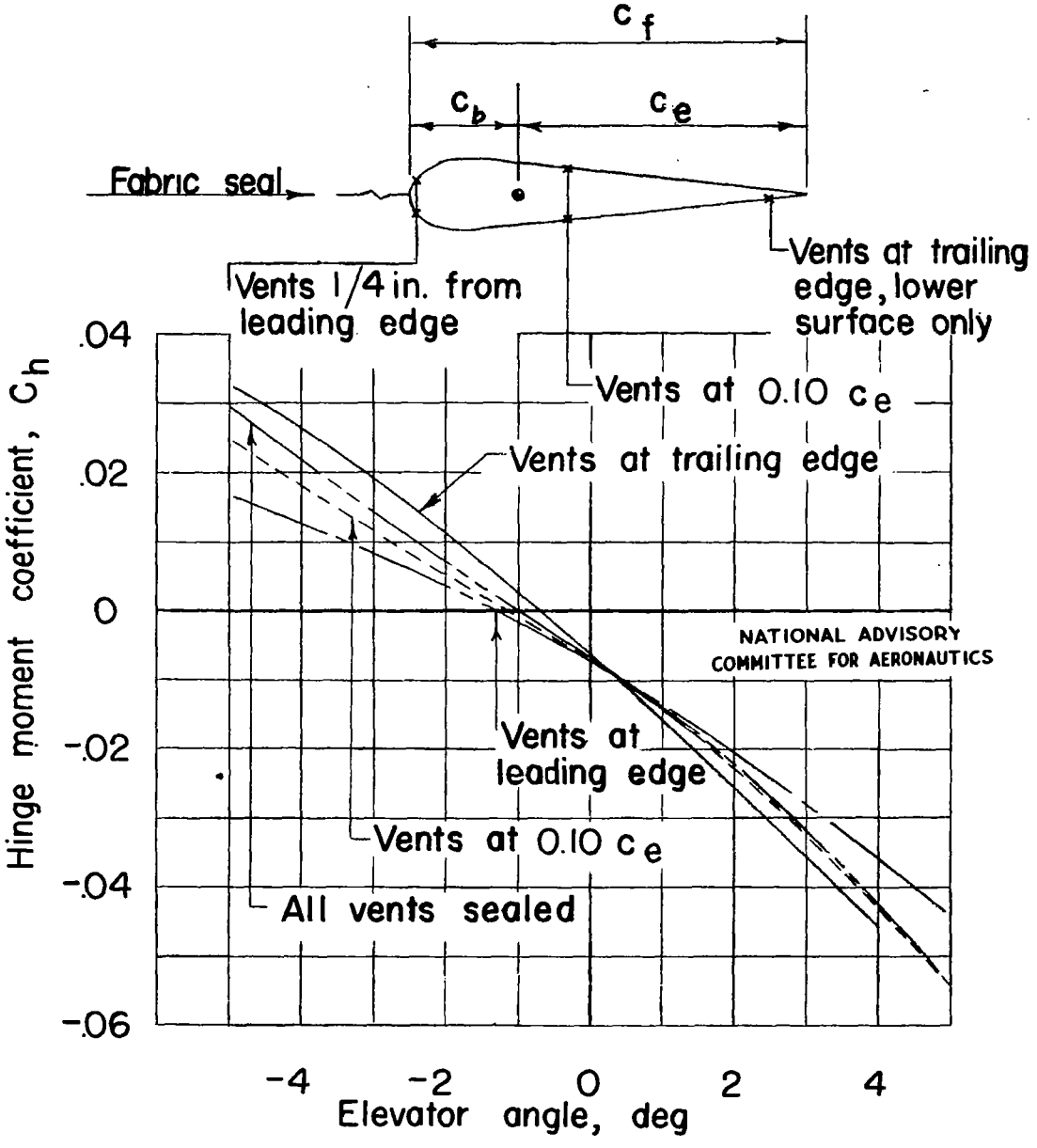

Figure 29 .—Effect of elevator vent location on elevator hinge moment; $\alpha = 0°$; M=0.55; elevator 2.

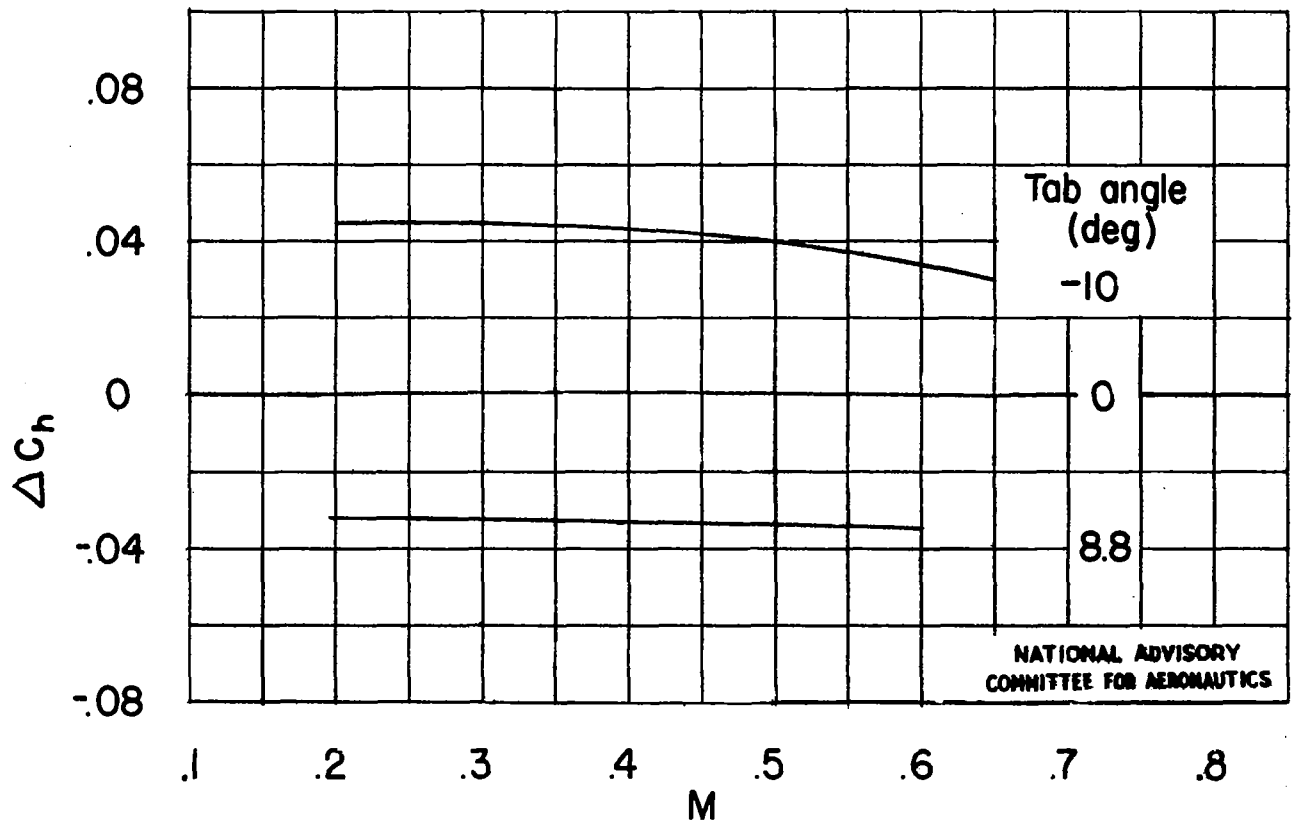

Figure 30 .— Effect of speed on trim-tab effectiveness. $\alpha = 0°; \delta = 0°$.